

Review of thermoelectric geometry and structure optimization for performance enhancement

 The corrections made in this section will be reviewed and approved by a journal production editor.

Samson Shittu^a, Guiqiang Li^{a,*} Guiqiang.Li@hull.ac.uk, Xudong Zhao^{a,b,*} Xudong.Zhao@hull.ac.uk,
Xiaoli Ma^a

^aCentre for Sustainable Energy Technologies, University of Hull, HU6 7RX, UK

^bDepartment of Power Engineering, North China Electric Power University, China

*Corresponding authors at: Department of Power Engineering, North China Electric Power University, China (X. Zhao).

Abstract

Thermoelectric geometry and structure optimization are vital research areas which are being explored extensively in recent years due to significant performance enhancement achieved. However, the lack of a single review paper on this key area is a huge gap identified. Therefore, this review presents a first of its kind in-depth analysis of the state of art in thermoelectric geometry and structure optimization. The four main parameters including leg length or height, cross-sectional area, number of legs and leg shape which are paid attention to during optimization of thermoelectric geometry are discussed in detail. In addition, a review of the different thermoelectric structure available in literature such as flat plate, annular, segmented, cascaded, corrugated, concentric, linear, flexible and micro thermoelectric generators and coolers is presented. Furthermore, special attention is paid to both electrical and mechanical performance enhancement obtainable from thermoelectric geometry and structure optimization. A review of thermal stress optimization is presented alongside other optimization including contact resistance, heat pipe, pulsed heating and cooling. Geometry and structure optimization methods including three-dimensional finite optimization and multi-objective optimization are discussed in detailed and the most significant results obtained from the literature review are presented. This comprehensive review will be a valuable and essential reference literature on all issues relating to thermoelectric geometry and structure optimization.

Keywords: Thermoelectric geometry; Thermal stress; Multi-objective optimization; Finite element method; Thermoelectric generator; Thermoelectric cooler

Nomenclature

I

Current, A

R	Resistance, Ω
T	Temperature, K
V	Voltage, V
ZT	Figure of merit

Greek symbols

α	Seebeck coefficient, V/K
κ	Thermal conductivity, W/m/K
σ	Electrical conductivity, S/m
η	Efficiency, %

Abbreviations

ATEG	Annular thermoelectric generator
Bi_2Te_3	Bismuth telluride
COP	Coefficient of performance
CoSb_3	Copper antimony
FDM	Finite difference method
FEM	Finite element method
FVM	Finite volume method
GA	Genetic algorithm
MOGA	Multi-objective genetic algorithm
NSGA-II	Non-dominated sorting genetic algorithm-II
PbTe	Lead telluride
PV	Photovoltaic
PV-TE	Photovoltaic-thermoelectric
SATEG	Segmented annular thermoelectric generator
SCGM	Simplified conjugate-gradient method
STEG	Segmented thermoelectric generator
TEC	Thermoelectric cooler
TEG	Thermoelectric generator

Subscripts

H	Hot side
C	Cold side

1 Introduction

Renewable energy is the future of global energy generation due to its superior advantage over the current conventional sources of energy like fossil fuel. In terms of safety and availability, renewable energy sources generate clean energy with zero pollution, and they are inexhaustible. The same cannot be said of conventional energy sources that cause serious environmental issues such as global warming and air pollution while being limited in supply. Therefore, it is only a matter of time before the numerous advantages offered by renewable energy sources outweigh the current limitations thereby ushering in a new era of sustainable energy. Availability

of electricity is a fundamental requirement for any society that seeks to thrive therefore, the current challenge is how to generate enough electricity to meet the increased energy demand without negatively affecting the environment. In addition, a high percentage of heat is wasted from vehicles, electrical instruments, human body, etc.

Thermoelectric (TE) devices can convert heat to electricity via the Seebeck effect or electricity to heat via the Peltier effect. They offer several advantages including zero pollution, compact size, silent operation, high reliability and absence of moving parts. Notwithstanding, the TE device has a low conversion efficiency which is the major disadvantage that has hindered the wide spread application of TE consequently, affecting its market growth in the area of electricity generation, heating, cooling and waste heat recovery. Furthermore, the cost of the thermoelectric material is currently too high to justify its low conversion efficiency. Therefore, the future of the TE is highly dependent on increasing its efficiency at a reduced cost. Consequently, a plethora of research is being undertaken on thermoelectric generator and cooler conversion efficiency improvement. A thermoelectric generator (TEG) is an energy converter capable of transforming heat to electricity via the Seebeck effect. This unique characteristic of the TEG makes it a valuable and indispensable technology for clean electricity generation. Furthermore, a thermoelectric cooler (TEC) operates according to the Peltier effect and can be used for cooling or heating.

In recent years, the two main methods being researched extensively for improving the TE efficiency while keeping the material cost low are geometry and material optimization. The goal of thermoelectric geometry research is to optimize the geometry and structure of the thermoelectric devices while thermoelectric material research entails developing new materials which possess a high value for figure of merit. Due to the significant results obtained from thermoelectric geometry optimization in the past, several researchers are now paying attention to this area therefore, the amount of available literature on this area has witnessed a sudden spike in recent years. Furthermore, the optimization of thermoelectric geometry and structure is imperative for the application of thermoelectric generators and coolers in areas with different heat source and heat sink shapes.

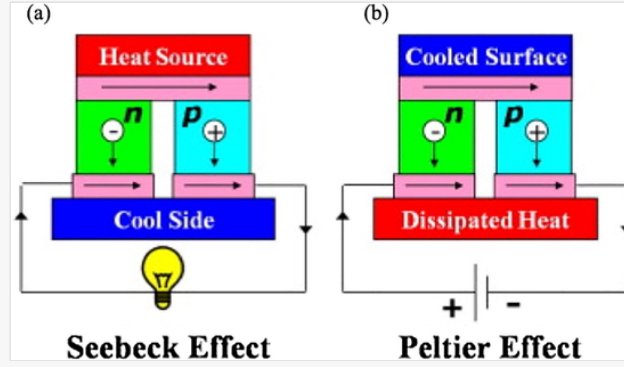
This review provides an in-depth analysis of the current research progress made in the area of thermoelectric geometry and structure optimization for performance enhancement of thermoelectric generators and coolers. The current state-of-art in TE geometry and structure research is explored in detail and the most significant results are presented. The objective of this review is to discuss all issues relating specifically to thermoelectric geometry and structure optimization. In fact, attention is paid not only to the electrical performance (efficiency and output/cooling power) improvement potential of the TE geometry and structure optimization research but also on the mechanical performance (thermal stress) enhancement obtainable by the optimization of thermoelectric geometry and structure. In addition, thermal stress developed in TE legs highly affect the life span of a TE device therefore; attention is paid to this important research area. Furthermore, different thermoelectric geometry and structure configuration are explored, and geometry optimization methods are discussed including three-dimensional finite optimization and multi-objective optimization methods. Lastly, future research directions are provided as a guide to interested researchers in the area of thermoelectric geometry and structure optimization.

2 Concept of thermoelectric generation and cooling

In the 18th century, the thermoelectric (TE) phenomenon was observed during the generation of small voltages between two dissimilar metals. Furthermore, the TE technology experienced a fast growth because of the invention of highly efficient semiconductors and because it offers specific advantages which made it different from the traditional energy generation and cooler [1]. A typical thermoelectric module is made up of p-type and

n-type semiconductor materials connected electrically in series and the presence of a temperature difference across its hot and cold side leads to the generation electricity generation [2]. Reversing current direction is a simple method to convert electricity into heating or cooling [3]. A thermoelectric device can convert heat directly into electricity via the Seebeck effect (Fig. 1 a) which was discovered in 1821 [4] while the Peltier effect (Fig. 1 b) which was discovered in 1834 allows the achievement of the reverse process (conversion of electricity to heat) [5]. Consequently, the bi-directional energy conversion capability of the thermoelectric device is shown in Fig. 1 [6].

Fig. 1



Schematic diagram showing principle of (a) Seebeck effect and (b) Peltier effect [6].

2.1 Thermoelectric material and application

Figure of merit (Z) is the most important parameter that determines the thermoelectric performance and it was discovered in 1911. Commonly, the figure of merit is made dimensionless by multiplying it with the absolute temperature (T) and this dimensionless figure of merit is expressed as [7]:

$$ZT = \alpha^2 \frac{\sigma T}{\kappa} \quad (1)$$

where σ is the electrical conductivity, κ is the thermal conductivity and α is the Seebeck coefficient. The inverse relationship between these intrinsic parameters makes it difficult to optimize one of the parameters without negatively affecting another parameter. This difficulty is the reason why the maximum figure of merit of thermoelectric material remained at at $ZT \approx 1$ for about fifty years [8]. Nevertheless, in-depth research on thermoelectric material being carried out as resulted in progress been reported in increasing TE figure of merit recently. The Seebeck coefficient is expressed as [9],

$$\alpha = \frac{\Delta V}{\Delta T} \quad (2)$$

where ΔT is temperature gradient and ΔV is electrostatic potential. Besides the Seebeck and Peltier effects, the last thermoelectric effect is the Thomson effect discovered in 1852 and it has a relationship with the reversion heat (q) generation rate. Furthermore, the current which flows through a portion of a single conductor with a

temperature gradient provides the reversible heat. The thermoelectric device performance is affected by Thomson effect and the accuracy of numerical studies can be improved by considering it [10].

Based on operating temperature, thermoelectric materials can be classified as high temperature (>900 K), medium temperature (500–900 K) and low temperature (<500 K). Applications which require high temperature need to use thermoelectric materials such as silicon-germanium alloys, applications which require medium temperature need to use thermoelectric materials which are based on group-IV tellurides including germanium telluride, tin telluride and lead telluride while bismuth telluride is used for low temperature applications [11]. For in-depth understanding of current thermoelectric material research, these two review papers [12] and [13] are recommended. The review papers have provided an in-depth review on thermoelectric material research therefore, for avoidance of repetition, the review papers are recommended for further reading.

In terms of application, thermoelectric generators have been applied for waste heat recovery in automobiles [14], low power generation [15], wearable sensors [16], space power [17] and medicine [18]. On the other hand, thermoelectric coolers have been applied for electronic device cooling, military, aerospace and medicine specific applications [19]. In addition, thermoelectric coolers have been used in refrigerators and air conditioners [20]. These two review papers [21] and [22] are recommended for in-depth understanding of current thermoelectric applications. A comprehensive review of thermoelectric applications has been provided in the recommended review papers.

2.2 Efficiency modelling

For an ideal thermoelectric device with constant thermoelectric properties, the thermoelectric generator maximum efficiency is expressed as [23],

$$\eta_{\max} = \eta_c \frac{\sqrt{1 + ZT} - 1}{\sqrt{1 + ZT} + \frac{T_C}{T_H}} \quad (3)$$

where the Carnot efficiency η_c is given as,

$$\eta_c = \frac{T_H - T_C}{T_H} \quad (4)$$

The thermoelectric cooler maximum efficiency is evaluated using coefficient of performance (COP) which is given as [23],

$$COP_{\max} = \frac{T_C \left[(1 + ZT)^{\frac{1}{2}} - \frac{T_H}{T_C} \right]}{(T_H - T_C) \left[(1 + ZT)^{\frac{1}{2}} + 1 \right]} \quad (5)$$

where T_H and T_C are the hot side and cold side temperatures respectively. ZT is the dimensionless thermoelectric figure of merit which is described in Eq. (1). The maximum thermoelectric conversion efficiency is limited by

the Carnot efficiency and the reduced efficiency which depends on the ZT , T_H and T_C .

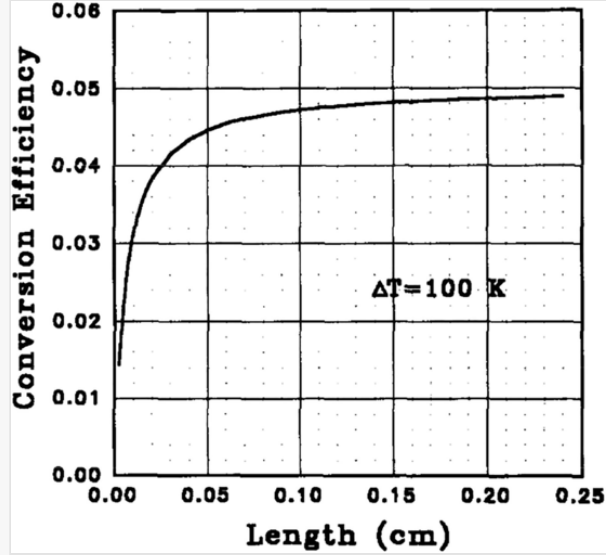
3 Thermoelectric geometry and structure optimization

Depending on the heat source and heat sink shape, thermoelectric devices could have different structures such as the conventional flat plate structure and annular structure. In addition, segmented structure can be adopted for high temperature applications and cascaded structure has been proposed. Furthermore, different geometries for the thermoelectric leg has been studied including conventional rectangular and asymmetrical geometries. The four main parameters which are paid attention to during optimization of thermoelectric geometry are leg length/height, cross-sectional area, number of legs and leg shape. Therefore, this section presents the optimization studies on these four parameters and a brief overview of the different thermoelectric structure currently being researched.

3.1 Leg length or height

The thermoelectric leg length or height is an important parameter which can be optimized for performance enhancement of the thermoelectric generator and cooler. Optimization of thermoelectric leg length has been performed in flat plate, annular, segmented and cascaded thermoelectric devices. In addition, the thermoelectric leg length has been optimized in a hybrid photovoltaic-thermoelectric system and enhanced performance was obtained. Min et al. [24] found that a decrease in thermoelectric leg length by 55% caused a 48% increase in power output and a 10% decrease in conversion efficiency as shown in Fig. 2. In addition, a theoretical investigation was carried out on three different commercial thermoelectric modules which only had different thermoelectric leg while other parameters were the same and a high temperature of 120 °C was considered on the hot side while the cold side was kept at ambient temperature. Kumar et al. [25] presented an optimization study on TE components for waste heat recovery in automobiles. Skutterudite thermoelectric material was used because it has a high figure of merit under high temperature conditions which is the application requirement for engines which operate on gasoline and diesel. Results showed that the leg efficiency was highly dependent on temperature difference, current and leg height. In addition, the authors argued that the careful selection of leg height and fill fraction enables the achievement of maximum power output while reducing the amount of material required.

Fig. 2

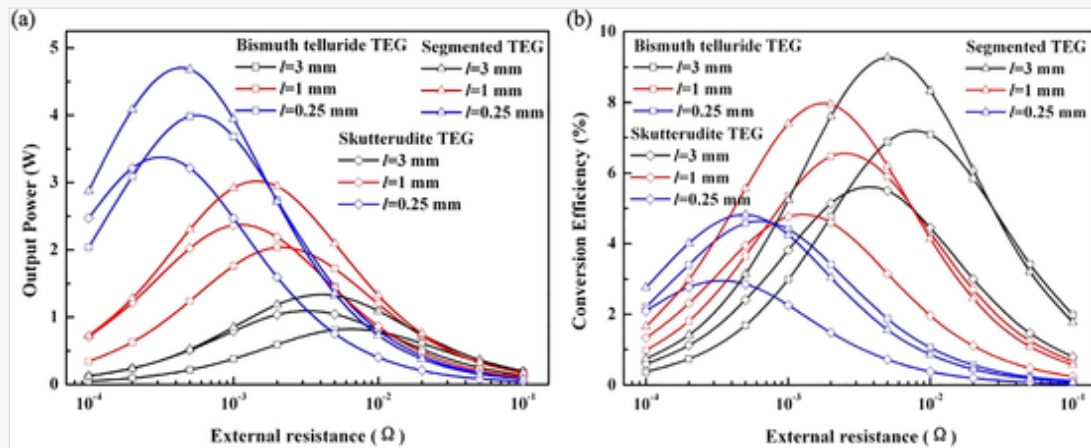


Variation of conversion efficiency with leg length [24].

Furthermore, Tian et al. [26] presented a detailed parametric optimization of a segmented thermoelectric generator (STEG) for diesel engine exhaust waste heat recovery and the authors recommended the use of STEG rather than traditional TEG especially for applications with high heat source temperature. In addition, results revealed that the highest TEG efficiency and power output had respectively, a linear and inverse relationship, with the thermoelectric leg length as shown in Fig. 3. It was also found that the enhanced performance obtained from the STEG compensated for the high thermoelectric material cost. Zhang et al. [27] optimized the leg length ratio of a STEG for power and efficiency enhancement and found the optimum leg length ratios for maximum efficiency and output power to be different. In addition, they found that the best ratio for thermoelectric leg length is determined by the thermoelectric material properties, geometry and conditions for heat transfer. Recently, Ma et al. [28] presented a detailed investigation on the optimization of STEG leg length ratio optimization for engine exhaust heat recovery. The STEG was optimized at component level and system level using a numerical model. Five different cases were considered corresponding to proportions of two materials in each case. The first two cases (Case 1 and Case) were the non-segmented conventional TEG while the remaining three cases corresponded to STEG with different leg length ratio. It was found that the optimal proportion of medium temperature material (CoSb_3) increased with longer thermoelectric legs and increased coefficient of heat transfer however, the leg area showed hardly any influence on it. In addition, results revealed that the application of optimal segmented ratio design in the TEG provided an enhanced performance and increased the power output by 6.8%. The maximum power output for both the segmented and non-segmented TEG increased as the heat source temperature increased (shown in Fig. 4). Recently, Shen et al. [29] studied the

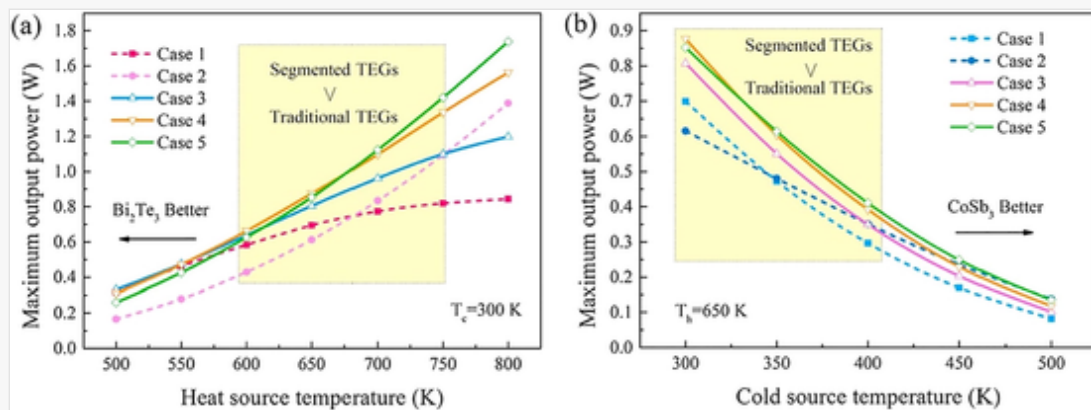
performance of a thermoelectric cooler with segmented configuration. They found that the maximum cooling capacity, maximum temperature difference and maximum coefficient of performance all decrease with the increase of leg length.

Fig. 3



Effect of leg length on (a) output power and (b) efficiency for three different thermoelectric generators [26].

Fig. 4



Maximum power output variation with (a) heat source and (b) cold source temperature [28].

Asides the optimization of thermoelectric leg length in flat plate and segmented thermoelectric devices, the idea of leg length optimization has also been utilized in annular thermoelectric devices. Shen et al. [30] studied the performance (power output and efficiency) of annular thermoelectric generator (ATEG) using a theoretical model and constant heat flux. Furthermore, the temperature dependency of TE materials was considered and the effect of shape parameter (S_r) on the ATEG output power was studied and they observed an increase in power output as thermoelectric leg length increased however, a reverse trend was observed under constant temperature condition. Zhang et al. [31] used a theoretical model to study the interface layers effect on ATEG performance and found that the interface layers negatively influenced the ATEG performance. Furthermore, they found that for ATEG with very short legs, the annular shape parameter significantly influences the ATEG performance. In addition, the simplified values used were found to provide results very similar to that of the real values. Furthermore, Shen et al. [32] investigated a segmented annular thermoelectric generator (SATEG) theoretically and a comparison with ATEG was presented. They found that the SATEG efficiency initially increased as the height ratios increased until it reaches a maximum after which it decreases. In addition, the authors observed that

temperature ratio increase caused an increase in the SATEG efficiency output power. Shittu et al. [33] investigated the SATEG mechanical and electrical performance using finite element method and a comparison with ATEG was presented. They observed a superior performance from the SATEG compared to the ATEG. In addition, results revealed that the leg length increase led to a decrease in TEG electrical performance.

The mechanical reliability and thermoelectric performance of SATEG was investigated by Fan et al. [34]. Results revealed that the SATEG output power increased initially before decreasing as the structural parameter increased. In addition, they found that the power output of the SATEG increased by 18.3% compared to that of the single-Skutterudite TEG. Asaadi et al. [35] studied a two-stage ATEG and found that the optimum height ratio required to obtain maximum thermodynamic and exergoeconomic efficiencies was directly influenced by the heat source intensity. In addition, results revealed that under certain heat source temperatures, the performance of the two-stage ATEG was superior to the performance of the single-stage ATEG however, the single-stage ATEG was more economical than the two-stage ATEG for all temperature of heat source considered. In a hybrid system like photovoltaic-thermoelectric (PV-TE), thermoelectric geometry optimization can enhance the hybrid system performance [36]. Hashim et al. [37] optimized the geometry of TE devices in a photovoltaic-thermoelectric system for output power enhancement. They argued in favour of considering the amount of thermoelectric material consumed during the optimization of the thermoelectric geometry for enhanced output power. It was also found that operating the PV-TE in a vacuum greatly increased its output power and they recommended the use of thermoelectric modules which had a smaller area than the area of photovoltaic.

Lamba et al. [38] studied the effect of TE geometry on the performance of a concentrated PV-TE system. They found that the thermoelectric leg length and temperature difference had an inverse relationship. Results also revealed that the concentrated PV-TE provided an enhanced output power and efficiency of 5% in comparison to those of the concentrated photovoltaic only system. Furthermore, Li et al. [39] also optimized the geometry of TE in a PV-TE. Results revealed that comparing the photovoltaic-thermoelectric and TE only systems, the optimum thermoelectric geometry in both systems are different. In addition, they found that the efficiency of the hybrid PV-TE decreased as the leg height increased. Mahmoudinezhad et al. [40] recommended TE geometry optimization in a PV-TE for output power enhancement. In addition, the authors performed a transient experimental and numerical study and found that the hybrid system thermal resistance increased with leg length. They also found that the ratio of the maximum power generated by the thermoelectric generator to the maximum power generated by the concentrating triple junction (CTJ) increased as the leg length increased. Recently, Cui et al. [41] optimized the leg height ratio in a segmented photovoltaic-thermoelectric system and found that the optimized height of the TE model which corresponds to the highest performance decreases with the height ratio of the upper to lower TE leg. In addition, they found that the optimized height of the TE model decreases with the concentrated solar irradiance.

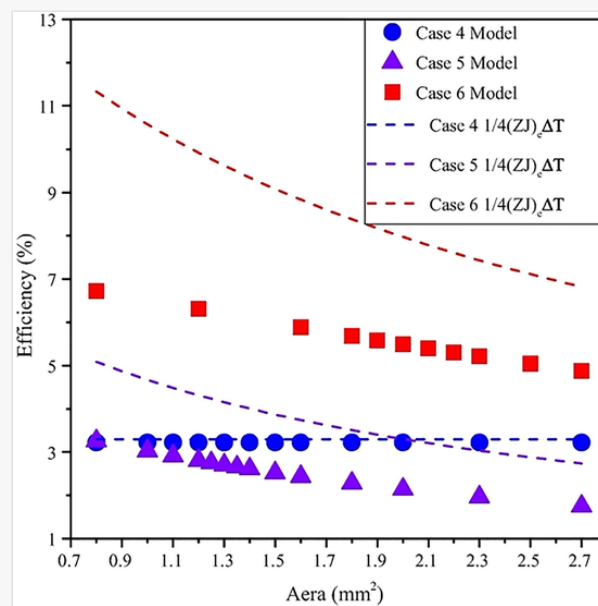
3.2 Leg cross-sectional area

Another important parameter which could be optimized for enhancing the performance of the thermoelectric generator and cooler is the leg cross-sectional area. Lavric [42] studied the sensitivity of TEG to geometry variation using a one-dimensional model and found that a higher power output can be obtained by using thermoelectric legs with larger cross-sectional area. Furthermore, the use of power density and output power per area for estimating the performance of TEG rather than output power and efficiency was recommended. In addition, it was found that decreasing contact resistances (electrical and thermal) could significantly increase the TEG performance. Cheng et al. [43] presented a structural optimization of thermoelectric modules and the effect

of TE leg area on the module performance was studied experimentally. The designed thermoelectric generator was for applications requiring low temperature such as waste heat recovery in hypersonic vehicles which has high heat flux from the scramjets. In addition, a polycrystalline bismuth telluride thermoelectric material was used, and results showed that maximum power output is obtainable at an optimum leg cross-sectional area.

Fan et al. [44] found the optimal thermoelectric leg area for enhanced TEG power output. At different thermal boundary conditions, the impact of geometric parameters on the TEG efficiency and output power density were analysed. Furthermore, the mathematical model used was validated with a previous numerical model and the authors argued that under specific thermal boundary conditions, the maximum power output can be obtained at an optimal leg cross-sectional area. In addition, they found that the thermoelectric conversion efficiency was almost constant at constant surface temperature boundary condition (case 4), while the efficiency was inversely proportional to the leg cross-sectional area at constant heat transfer coefficient boundary condition (case 5 and 6) as shown in Fig. 5. He et al. [45] presented a comprehensive one-dimensional model for thermoelectric generator module geometric optimization based on the Hill-climbing algorithm for power output enhancement. Numerical simulations carried out considered the impact of the dimensions of thermoelectric legs on the thermoelectric generator performance. Furthermore, the Seebeck, Thomson and Peltier effects were considered in the one-dimensional mathematical model presented which was validated with a three-dimensional numerical model and it was found that for any given leg length, the maximum power output always increases as the leg area increases.

Fig. 5



Conversion efficiency variation with leg cross-sectional areas [44].

Furthermore, using a theoretical model, Zhang et al. [46] investigated the effect of the geometry of ATEG legs on system performance. Results revealed that the performance of the ATEG and flat plate TEG were similar when the TE leg cross-sectional area configuration was kept constant. In addition, results showed that the maximum power output per unit mass could be obtained only when the leg cross-sectional area is constant for the ideal ATEG. Cui et al. [47] studied the potential of porous ATEG for utilization of waste heat and observed a superior performance from the porous ATEG compared to the bulk TEG. In addition, thermal and electrical contact resistances were considered and using a theoretical model, they found that the TEG output power had a linear relationship with temperature difference and an inverse relationship with cross-sectional area. Furthermore, Nemati et al. [48] studied a two-stage TEC that was separated electrically and found that the optimization of leg

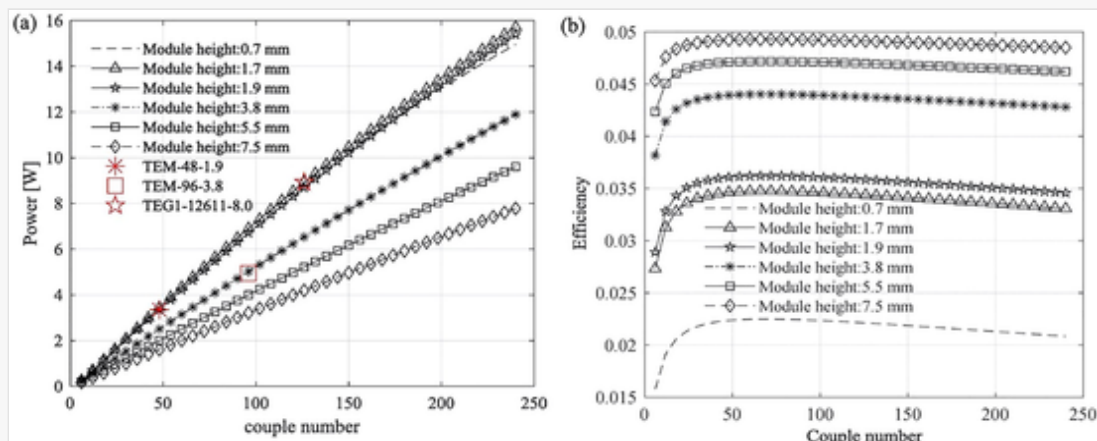
area ratio enhanced the cooling power cost and exergy efficiency. Results also revealed that the second stage applied current must be higher than that of the first stage to obtain maximum exergy efficiency at the lowest possible cost of cooling. In addition, they found that the optimum cross-sectional area ratio is less than unity.

A three-dimensional model was utilized by Shittu et al. [49] to investigate the optimum geometry for thermoelectric devices in a hybrid system for enhancing the efficiency of the PV-TE. Different configurations were considered corresponding to different geometries and results revealed that the type of PV cell used could influence the best geometry for TE in a hybrid system. In addition, they found that the hybrid PV-TE efficiency increased as the leg cross-sectional area increased. Li et al. [50] investigated the optimum leg cross-sectional area in a hybrid PV-TE system. Results showed that the hybrid PV-TE system attained its highest power output when $A_n/A_p = 1$ while this is different for the thermoelectric only system which attains its highest power output when $A_n/A_p < 1$. In a subsequent study [51], the same authors found that the overall efficiency of the hybrid PV-TE increases when a larger thermoelectric leg cross-sectional area is used.

3.3 Number of thermoelectric legs

Dongxu et al. [52] performed an experimental and numerical study on thermoelectric module geometry optimization for power output enhancement at a low cost. Three thermoelectric modules with different geometries but same material were analysed experimentally, and the simulation model was validated with experimental results. The effect of thermoelectric module couple number on the power output and efficiency of the module was studied. Results obtained (shown in Fig. 6) revealed that the power output monotonically increases as the leg number increases due to the decrease in thermal and electrical contact resistances. In addition, they found that the efficiency first increases and then decreases as the leg number is increased. Furthermore, Hodes [53] presented a method to optimize the thermoelectric leg number for obtaining maximum power output and conversion efficiency for a specified performance. The load resistance was optimized for obtaining best performance using a specific leg geometry. In addition, a comparison of thermoelectric geometry optimization in power generation and refrigeration/cooling modes was presented. Results showed that in refrigeration mode, the number of thermoelectric legs affects neither the performance or efficiency however, in generation mode, both the number of thermoelectric legs and height of thermoelectric legs must be optimized simultaneously when both power output and load resistance are specified.

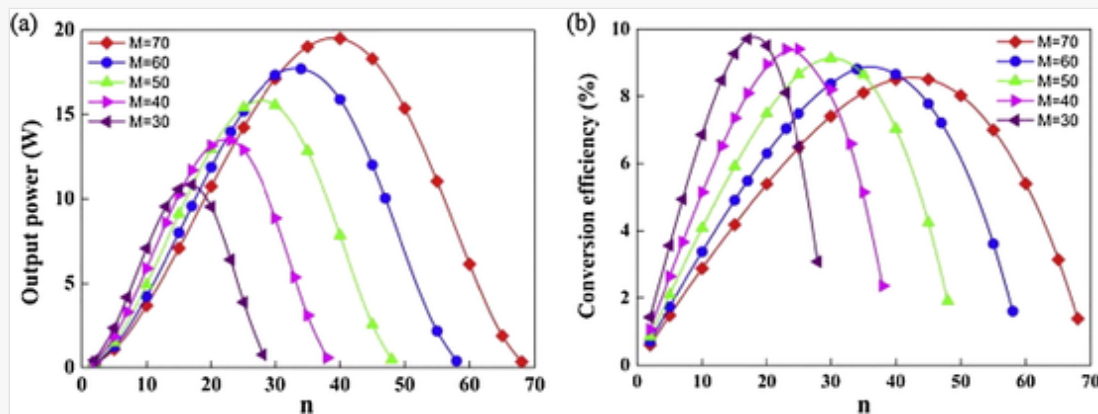
Fig. 6



Variation of leg number with (a) power output and (b) efficiency [52].

Liang et al. [54] optimized a two-stage TEG and compared it with a single TEG. They found that the absorbed heat and output power increased as the total number of thermoelectric legs increased however, the conversion efficiency decreased. In addition, they found that the temperature of the heat source had a greater effect on the performance of the TEG compared to the temperature of the cold source. The relationship between the total number of thermoelectric legs (M), number of thermoelectric legs in bottom stage (n), output power and efficiency of the two-stage TEG is shown in Fig. 7. It was found that the increase of M caused an increase in the maximum optimum output power and a decrease in the conversion efficiency. Wang et al. [55] optimized three different two-stage thermoelectric cooler (TEC). They found that the hot stage thermoelectric leg number should be higher than the cold stage thermoelectric leg number to obtain enhanced coefficient of performance and cooling capacity. Furthermore, the authors argued that accurate two-stage TEC performance prediction is only possible by the use of thermoelectric materials properties which are dependent on temperature. Yin et al. [56] studied the effect of leg number on the performance of a solar thermoelectric generator under non-uniform solar radiation. The authors argued that reducing the thermoelectric leg number is an effective method to increase the performance of thermoelectric generator under non-uniform solar illumination. They found that under the same non-uniform solar radiation, the maximum power output increased by 73.5% when the leg number decreased from 32 to 18 and it increased by 244.9% when the leg number decreased from 32 to 8.

Fig. 7



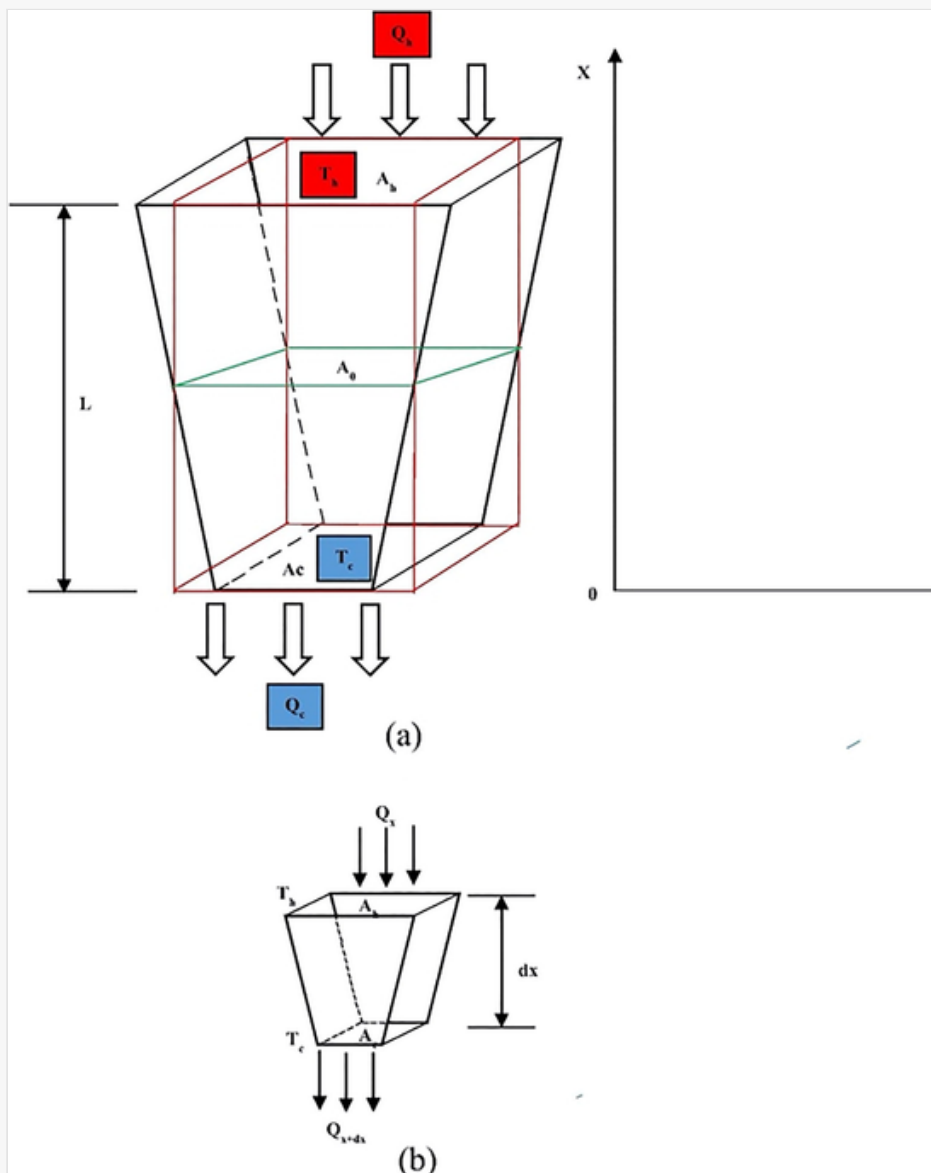
Relationship between number of legs and (a) output power and (b) conversion efficiency [54].

Recently, Luo et al. [57] recommended the use of more thermoelectric legs to achieve a greater power output from the TEG. In addition, they found that the maximum power output and maximum efficiency of the thermoelectric module with increased thermoelectric leg number increased by 1% and 1.2% respectively. Miao et al. [58] analysed and optimized the mechanical stability of thermoelectric modules. In addition, the influence of the number of thermoelectric legs on the stability of the thermoelectric module was studied and they found that optimization of the thermoelectric leg number can reduce the internal stress generated in the module and improve the working stability of the module. Furthermore, the effect of TE leg number on the PV-TE performance was investigated by Lakeh et al. [59]. A parametric study was performed, and they found that the PV-TE efficiency for any given length of arms would have an optimum range versus different number of TE legs. It was also found that the PV-TE could be advantageous when used in conditions of outer space or by adding a heat absorber to the hybrid system.

3.4 Thermoelectric leg shape

The conventional thermoelectric legs are rectangular/symmetrical however, asymmetrical thermoelectric legs are being researched as a method to improve the transfer of heat in the legs and enhance the TE performance. In fact, the TE legs temperature gradient can be increased due to the reduction of the TEG overall thermal conductance which is achieved by using asymmetrical legs. Furthermore, asymmetrical thermoelectric legs usually have variable cross-sectional area resulting in a trapezoid shape. Sahin et al. [60] studied theoretically, the effect of thermoelectric geometry on the performance of a TEG. A TEG which had variable cross-section legs was studied and they found that the trapezoid shape leg geometry significantly improved the TEG efficiency. In addition, they found that the power generation capability of the TEG was greatly affected negatively by the shape parameter. Similarly, a thermodynamic model was used by Ali et al. [61] to study the influence of TE geometry on the thermal performance of TEG. Results revealed that the increase of the geometric parameter which is dimensionless caused an improvement in the thermal efficiency of the TEG. In addition, they found that the point at which the highest efficiency was obtained was different from the point at which the highest power output was obtained. The influence of TE geometry configuration on the TEG (shown in Fig. 8) performance was studied by Lamba et al. [62]. They found that the exergy and energy efficiency of the trapezoidal shaped TEG increased by 2.31% and 2.32% respectively. In addition, they found that the point at which highest output power was obtained was different from that at which the highest exergy and energy efficiency was obtained.

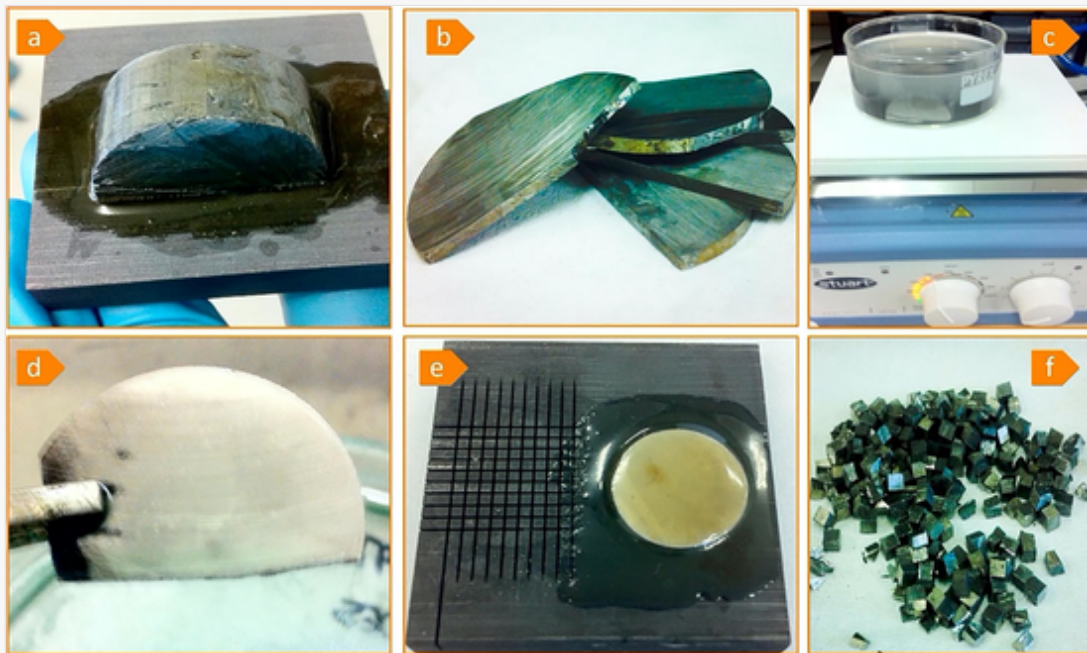
Fig. 8



(a) Schematic of leg, rectangular area is shown in red colour and (b) cross-sectional view of trapezoidal TEG [62]. (For interpretation of the references to colour in this figure legend, the reader is referred to the web version of this article.)

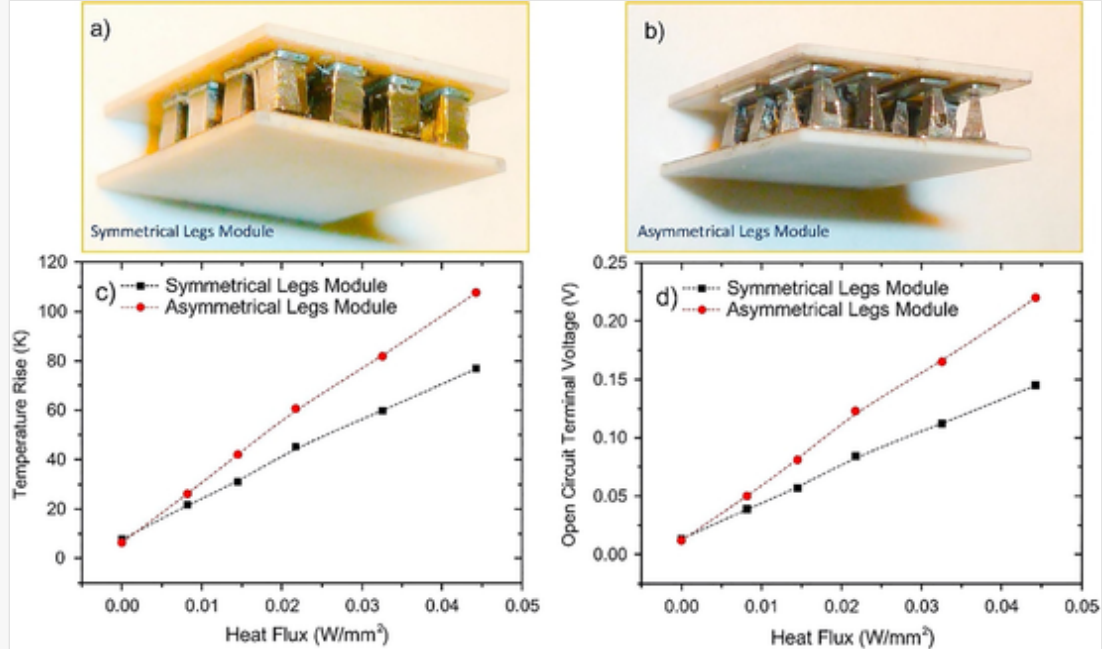
Furthermore, Shi et al. [63] studied the optimum TE leg geometry and investigated the effect of shape parameter on system performance. They found that when both nominal power density and efficiency are essential, TEGs with trapezoidal legs are better. In addition, they found that at a zero value for shape parameter, the highest nominal power density could be obtained. Fabián-Mijangos [64] investigated numerically and experimentally, thermoelectric generators with asymmetrical legs. Fig. 9 shows the thermoelectric legs fabrication process while Fig. 10 demonstrates the superiority of the asymmetrical legs in comparison to the symmetrical legs. This study provided the first experimental prove of concept which showed the feasibility of asymmetrical thermoelectric legs for performance enhancement. Lin et al. [65] optimized a two-stage trapezoid shaped TEC. Intermediate ceramic plates were eliminated to reduce the inter-stage thermal resistance and enhance performance. They found that the two-stage TEC coefficient of performance and maximum cooling capacity were affected by the hot-stage trapezoid leg shape ratio. Similarly, Lamba et al. [66] studied a thermoelectric cooler using a thermodynamic model and found that the TEC cooling capacity increased because of Thomson effect. Furthermore, they found that the best values for the shape parameter and the load ratio were respectively 1 and 2 at which the highest output power could be obtained.

Fig. 9



Fabrication steps for thermoelectric legs [64].

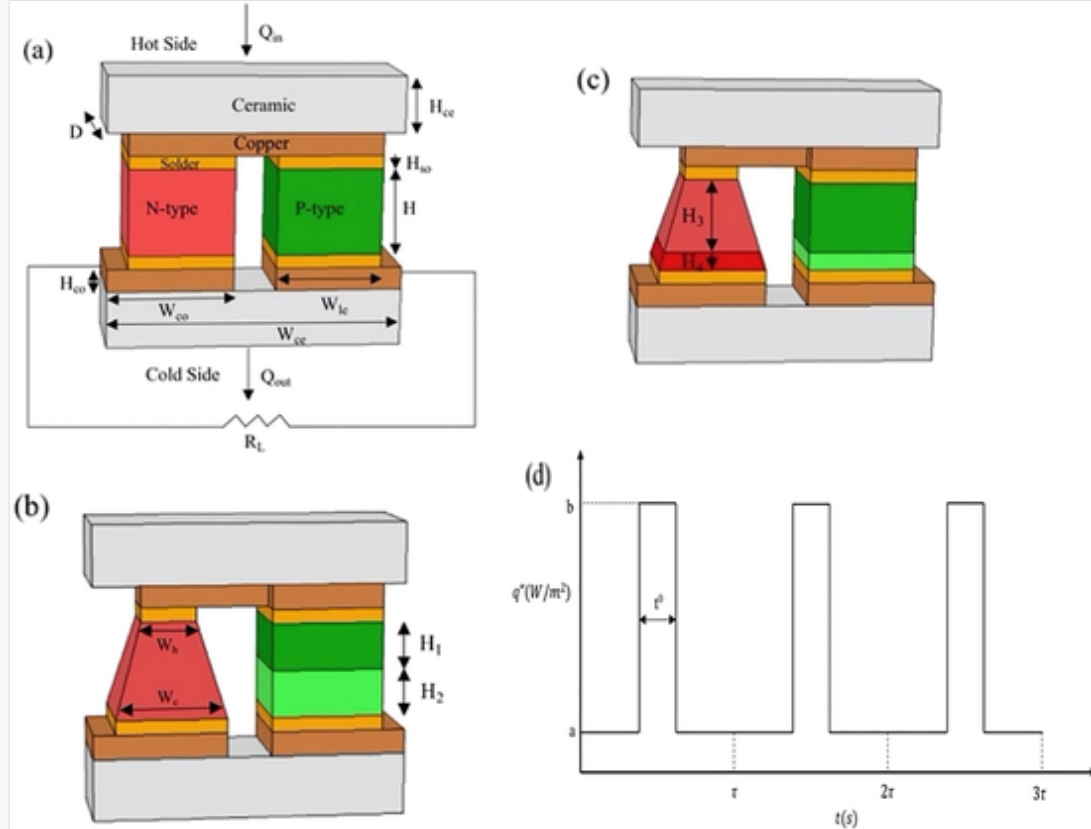
Fig. 10



Fabricated module (a) with symmetrical legs (b) with asymmetrical legs (c) temperature difference (d) open circuit voltage [64]

Liu et al. [67] presented a novel solar thermoelectric generator design which had thermoelectric materials that were segmented and thermoelectric legs with asymmetrical geometry. The numerical study was performed using a three-dimensional model and the leg area and length ratios were optimized. They found that the use of asymmetrical legs with the segmented design enabled a 4.21% additional power output enhancement in comparison to the optimized segmented legs without asymmetrical geometry. Similarly, Shittu et al. [68] presented a detailed numerical study on a TEG with segmented and asymmetrical legs (shown in Fig. 11) under transient and steady state conditions. A comparison with non-segmented TEG was presented and the new design of TEG was optimized for electrical performance and mechanical reliability enhancement. In addition, rectangular pulsed heat power was applied as the heat source for performance enhancement. Results showed the superior performance of the optimized design in comparison with the traditional TEG. Furthermore, a segmented asymmetrical TEG was studied by Karana et al. [69] and they investigated geometric parameter effect on the system performance. Results from the theoretical study showed that the geometric parameter strongly influenced the load ratio and temperature ratio. In addition, the authors argued that due to advancement in the technology required to manufacture the TE legs, the new unconventional shape of the TE leg could be made more cost effective. The power generation capability of the newly designed TEG was observed to be higher than that of the traditional TEG.

Fig. 11



Schematic of (a) non-segmented TEG (b) segmented asymmetrical TEG (c) optimized geometry and (d) rectangular pulse heat [68].

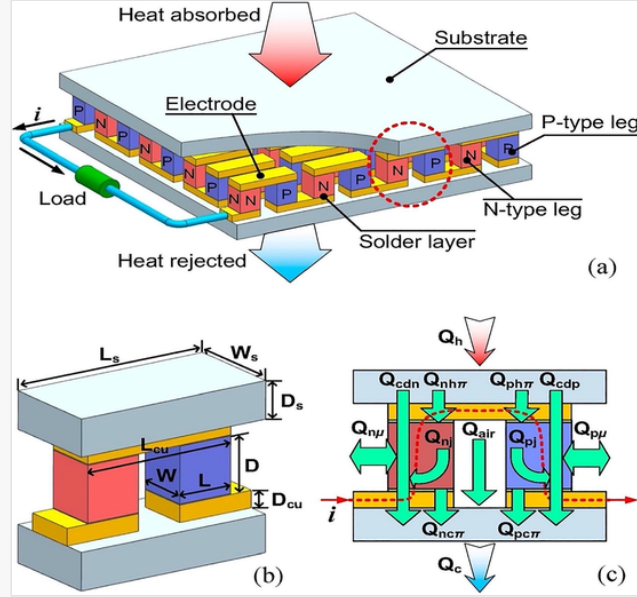
3.5 Thermoelectric structure

This section presents a brief overview of the different thermoelectric structure currently being researched and some of the results obtained using these structures.

3.5.1 Flat plate thermoelectric

The most common and conventional structure of a thermoelectric module is the flat plate as shown in Fig. 12 [45]. As shown, a thermoelectric module consists mainly of ceramic substrate, copper electrode, solder layer and semiconductor thermoelectric legs which are usually connected in parallel thermally and in series electrically. Thermal and electrical contacts are usually present in a thermoelectric module with thermal contact existing between the copper surface and the ceramic surface while electrical contact occurs between the thermoelectric leg surface and the copper surface. The ceramic substrate provides thermal conductivity and electric insulation while the copper electrode provides the electrical connectivity. The solder layer connects the copper layer and thermoelectric legs while also helping to decrease thermal stress effect. The choice of thermoelectric material is greatly influenced by the specific application and operating temperature. Furthermore, the TE module has two sides including hot side and cold side and depending on required, the TE can be operated as a generator (TEG) to produce electric power to an external load or as a cooler (TEC) for cooling/heating. In terms of geometry optimization, the TE leg area and length are usually paid more attention, in addition to the thickness of the copper, solder and ceramic layers.

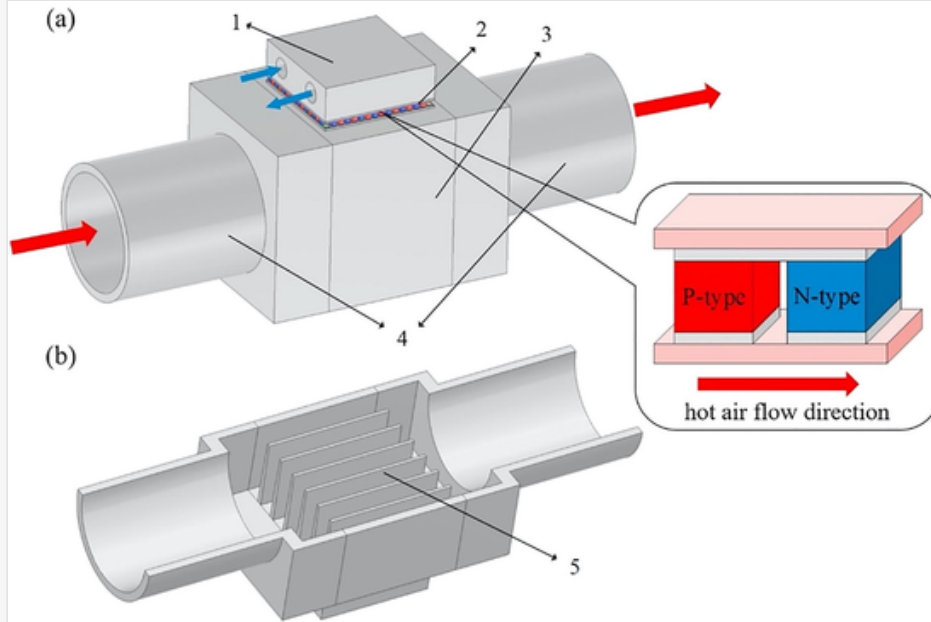
Fig. 12



Schematic of (a) thermoelectric generator (b) thermoelectric uni-couple and (c) energy flow diagram [45].

Luo et al. [70] presented a novel thermoelectric module structure (shown in Fig. 13). A numerical and experimental study was carried out and results showed the new TE module structure had a superior performance than the traditional TE module using the same material quantity. In addition, the thermoelectric material used was based on BiSbTeSe and a steady state numerical study was carried out. The authors found that the ratio of load resistance to internal resistance is greater than one for obtaining maximum output power. He et al. [71] optimized the design of a TEG for use as an engine waste heat recovery system and argued that improved TEG performance can be achieved by optimizing the module area. In addition, the impact of the parameters of the exhaust gas on the thermoelectric generator optimum performance was investigated and found that the best module area is affected greatly by the mass flow rate. Using dimensional analysis, Lee [72] presented an optimal design of thermoelectric devices for obtaining maximum efficiency (or COP) and power output (or cooling power). Therefore, both a thermoelectric generator and cooler was optimized, and the authors argued parameters such as load resistance ratio, thermal conduction ratio, efficiency and power could be obtained in dimensionless form using the optimal design. In addition, the heat sink was also optimized, and the best ratio for load resistance was found to be greater than one, for a thermoelectric generator with heat sink.

Fig. 13

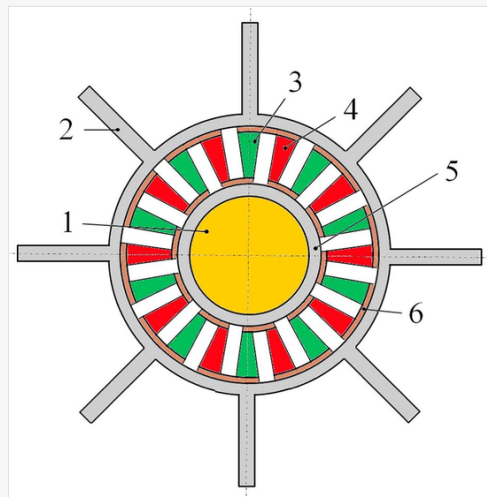


Thermoelectric generator structure (a) main view and (b) cutaway view. Where (1) heat sink (2) thermoelectric module (3) heat exchanger (4) heat exchanger inlet and outlet connectors and (5) heat exchanger inner fins [70].

3.5.2 Annular thermoelectric

When circular heat sinks or heat source are to be used, annular thermoelectric modules are beneficial as shown in Fig. 14 [46]. This is because they can eliminate any contact resistance resulting from mismatch of geometry. Applications with a radial heat flow or cylindrical heat source would require a different type of thermoelectric configuration besides the conventional flat plate thermoelectric configuration which would be unsuitable in such applications [73]. Bauknecht et al. [74] analysed the performance of annular thermoelectric couples under non-uniform temperature distribution. Contact resistances and parasitic effects in the thermoelectric module were considered and results showed that uniform temperature distribution provides a better performance. Furthermore, Kaushik et al. [75] investigated an annular thermoelectric generator (ATEG) and provided expressions for the optimum current at which the highest output power could be obtained. In addition, the figure of merit expression was modified while considering the Thomson effect. The simulation was performed using a Simulink block diagram and they found that the ATEG provided a lower performance than the flat plate TEG. Furthermore, results revealed that the consideration of Thomson effect caused the ATEG performance to be decreased.

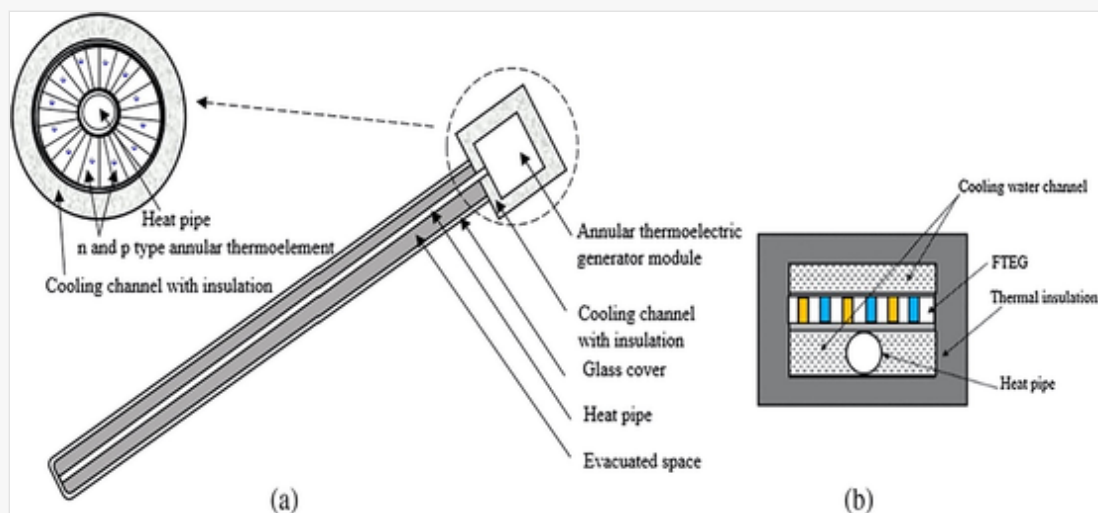
Fig. 14



Schematic diagram of ATEG: (1) heat source (2) heat sink (3) p-type leg (4) n-type leg (5) ceramic (6) copper electrode [46].

Similarly, Manikandan et al. [76] analysed the performance of ATEG with solar heat pipe shown in Fig. 15. They found that in addition to the solar ATEG providing better performance compared to the flat plate TEG, it also provides improved heat transfer characteristics. Furthermore, the authors argued that the new solar ATEG could be installed and maintained easily in comparison to the flat plate TEG due to its structure which is cylindrical in natural. However, they also stated that the solar ATEG systems are not economical although an increase in thermoelectric figure of merit would make such systems more attractive. Shen et al. [77] presented a one-dimensional steady state model to analyse an ATEG performance. They found that the ATEG and flat plate TEG operate using similar fundamental formulas with the only difference being the total electrical resistance and thermal conductance expressions. In addition, when the annular shaped parameter is 1, the ATEG turns into a flat plate TEG.

Fig. 15



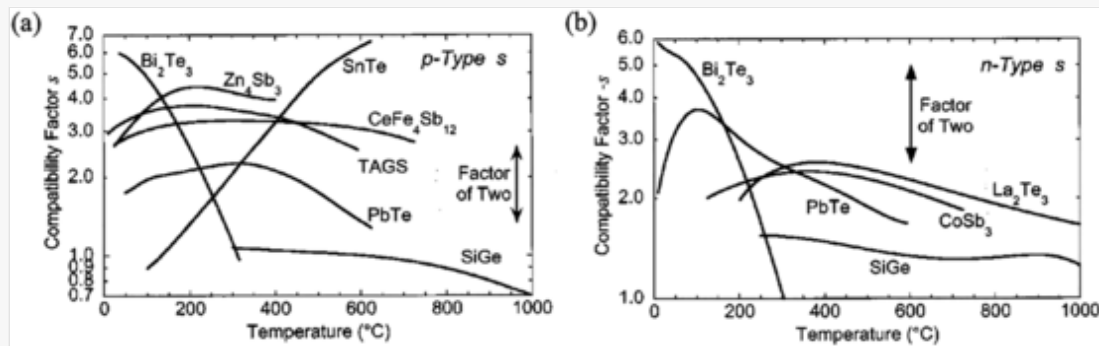
(a) Solar heat pipe annular TEG and (b) cross-sectional view of solar heat pipe flat plate TEG [76].

3.5.3 Segmented thermoelectric

Since thermoelectric materials are only efficient in specific temperature ranges, the idea of segmented thermoelectric generator and cooler has attracted more interest recently. The reason for this is that, materials that

are highly efficient at specific temperature ranges can be combined due to segmentation. For example, highly efficient medium temperature range thermoelectric material (CoSb_3) can be combined with a low temperature range TE material with high efficiency (Bi_2Te_3). Consequently, the two materials will function in the temperature range in which they are most efficient thereby leading to an enhanced overall performance. However, not all thermoelectric materials are compatible [78] therefore, the compatibility factor must be considered because for a segmented thermoelectric, it is the most important parameter as thermoelectric material properties are subject to change from one segment to another [79]. Fig. 16 shows the compatibility factor (s) for thermoelectric materials. When the relative current density ($u = J/\kappa\nabla T$) is equal to the compatibility factor ($s = (\sqrt{1 + zT} - 1)/\alpha T$), maximum conversion efficiency can be achieved [80]. Consequently, segmentation will become inefficient if the compatibility factor differs by a factor of 2 or more [79]. Generally, spark plasma sintering (SPS) method is used to fabricate most non-segmented and segmented thermoelectric materials because it is less time consuming and it provides improved thermoelectric material performance [81].

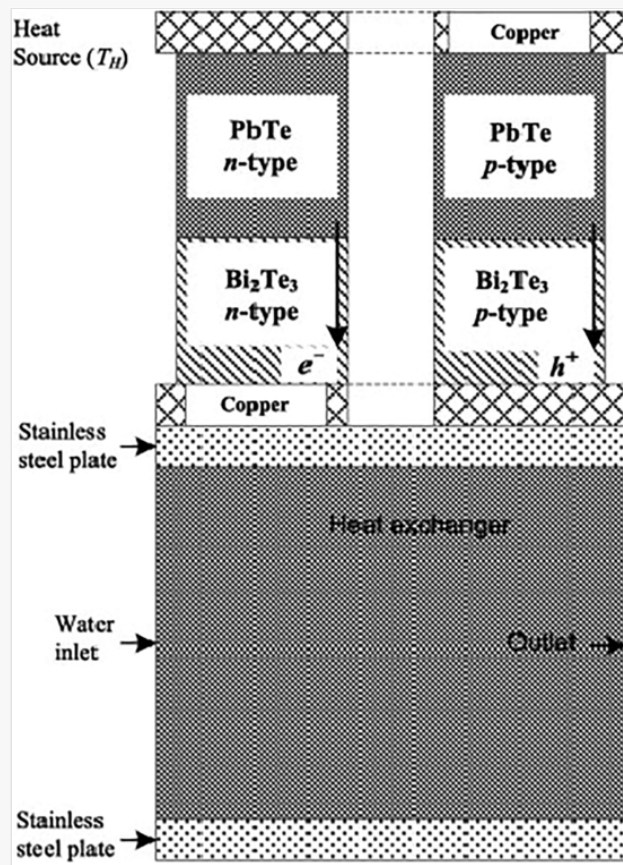
Fig. 16



Compatibility factor (s) for (a) p-type and (b) n-type thermoelectric materials [79].

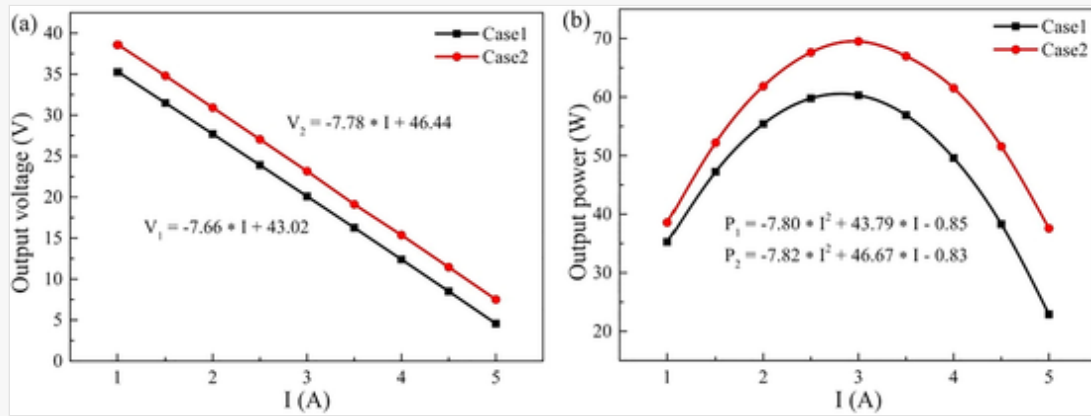
Hadjistassou et al. [82] presented a methodology formulated on computation and analytical modelling for designing highly efficient segmented thermoelectric generator (STEG) shown in Fig. 17 and found that the STEG achieved a 5.29% maximum efficiency at a 324.6 K temperature gradient. In addition, they found that the STEG thermal resistance increased as the TEG temperature difference increased and the thermoelectric materials used were bismuth telluride and lead telluride. Kim et al. [83] studied the behaviour of a two-pair STEG which could be used for recovering waste heat in unmanned aerial vehicles and observed that the use of low electrical barriers improved the STEG performance. Shu et al. [84] analysed the STEG and TEG performance for diesel engine waste heat recovery. As shown in Fig. 18, the results revealed a 13.4% increase in the solar thermoelectric generator maximum output power compared to that of the TEG. The authors recommended the use of STEG for waste heat recovery as it was more effective. Furthermore, they found that the heat sink fins affect the best thermoelectric module configuration. The design of a STEG with high performance and with cost considered was presented by Ouyang et al. [85] and contact resistances (electrical and thermal) were accounted for. Different combinations of segmented thermoelectric legs were considered and the most efficient geometry with the best cost performance ratio were analysed as shown in Fig. 19. The thermoelectric figure of merit was argued by the authors as the top criterion to be considered when choosing TE materials.

Fig. 17



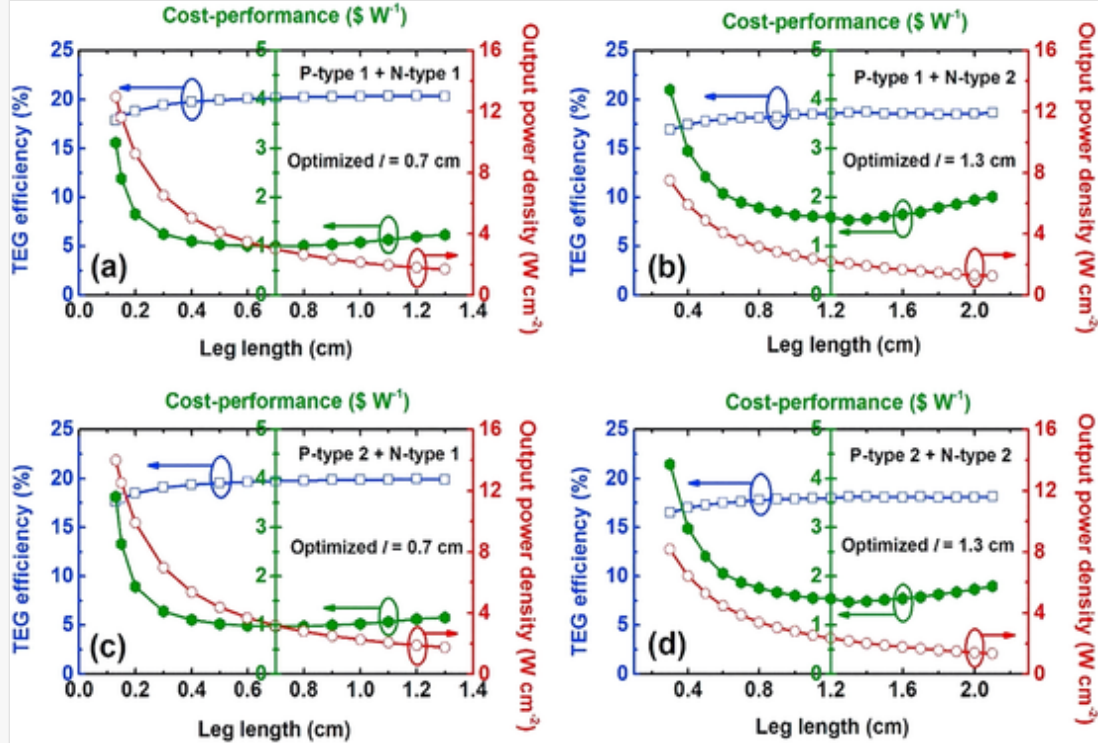
Schematic of STEG with active cooling heat exchanger [82].

Fig. 18



(a) Voltage output and (b) Power output of non-segmented (case 1) and segmented TEG (case 2) [84].

Fig. 19



Cost performance ratios, TEG efficiencies and power output densities versus leg lengths of different TEG modules [85].

3.5.4 Cascaded thermoelectric

Unlike in a segmented thermoelectric generator or cooler, the issue of compatibility can be avoided by cascading rather than segmenting a TEG or TEC because in principle, for each stage of a cascaded thermoelectric device, the electrical circuits are independent therefore, for each stage, the best relative current density values can be used even if they are different [79]. Cascaded thermoelectric devices are also called multi-stage thermoelectric devices because multiple thermoelectric modules are usually placed directly on each other in a cascaded form. Xiao et al. [86] studied a cascaded TEG with two-stage and three-stage. They found that the three-stage TEG achieved an efficiency of 10.52% and the performance comparison results of the TEG with different stages is shown in Table 1. The thermoelectric materials used were bismuth telluride and Skutterudite and the authors argued in favour of STEG as new thermoelectric materials are developed with high figure of merit.

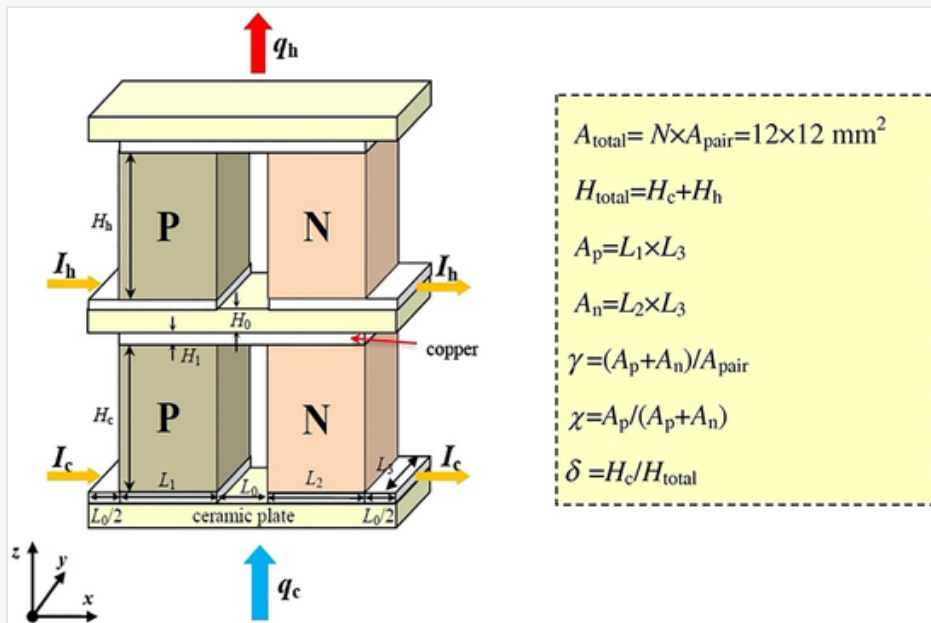
Table 1

i The table layout displayed in this section is not how it will appear in the final version. The representation below is solely purposed for providing corrections to the table. To preview the actual presentation of the table, please view the Proof.

Uni-couple	Single-stage (Bi2Te3)	Two-stage	Three-stage
Concentration ratio	168	173	179
Input power (W)	0.2579	0.2652	0.2749
Output power (W)	0.0279	0.0353	0.0452
Efficiency (%)	10.82	13.31	16.44

Cheng et al. [87] analysed the performance of multi-stage and single-stage TEGs. Results showed that the multi-stage TEG which was cascaded provided an enhanced performance [87]. In addition, the authors found that the superiority of the multi-stage TEG over the single-stage TEG becomes more obvious at large temperature differences [88]. Similarly, Wang et al. [89] optimized a two-stage TEC (shown in Fig. 20) and found that the optimal design could be obtained at specific temperature difference due to the temperature difference independence of the applied current and geometric structure. Furthermore, Lv et al. [90] investigated a two-stage thermoelectric cooler and noticed that for the two-stage TEC, the maximum temperature drop at the cold side increased significantly compared to the single-stage TEC. In addition, they argued that pulse and geometry optimization improved the temperature overshoot, super cooling state holding time and cold side maximum temperature decrease.

Fig. 20



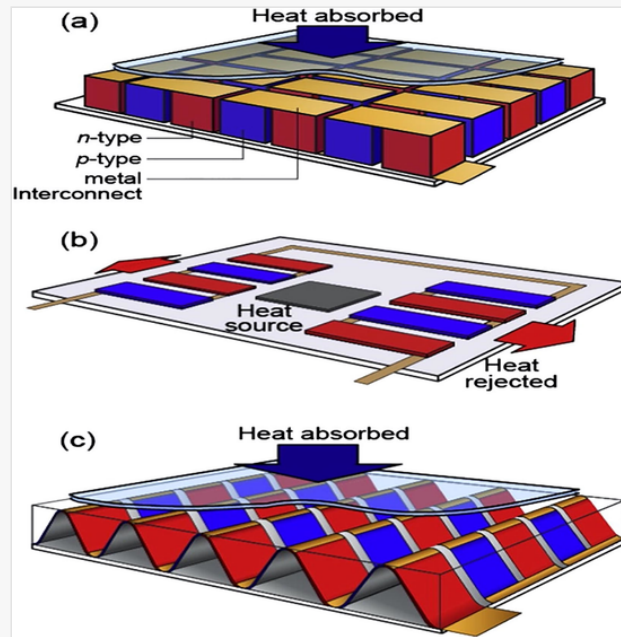
Two-stage TEC symmetric unit with separate applied current configuration [89].

3.5.5 Corrugated, concentric and linear thermoelectric

In this section, the few research available on corrugated, concentric and linear thermoelectric devices are presented. Firstly, Owoyele et al. [91] presented a novel thermoelectric cooler (TEC) architecture (shown in Fig. 21). The effects of various geometry parameters were studied, and they found that the corrugated TEC performed better and was competitive in terms of cost for applications with low cooling power density. In addition, the authors recommended the use of corrugated TEC for applications which required a low cooling power density over a large area. Appropriate thickness selection was also recommended for reducing losses in a

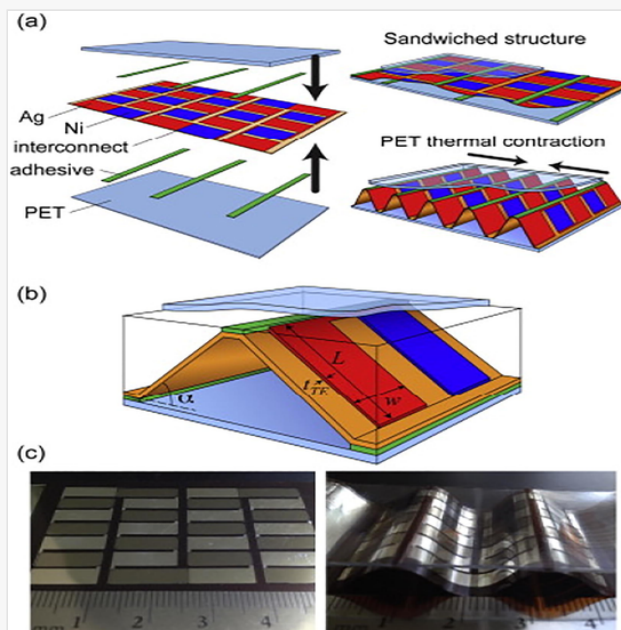
corrugated TEC. Furthermore, Sun et al. [92] studied a TEG which was made up of thin film and corrugated architecture. Fig. 22 shows the process for fabricating the corrugated structure of the TEG. They found that the heat-shrink fabrication approach which was used was simple and better for applications with large area and low power density. In addition, the authors argued that the corrugated TEG was more economic for applications which required small power density, and which used low quality waste heat as the heat source. Furthermore, they stated that the use of thermal interface layers which had high values of thermal conductivity would lead to an increase in the TEG performance.

Fig. 21



Schematic of (a) conventional flat plate TEC (b) in-plane TEC and (c) corrugated TEC [91].

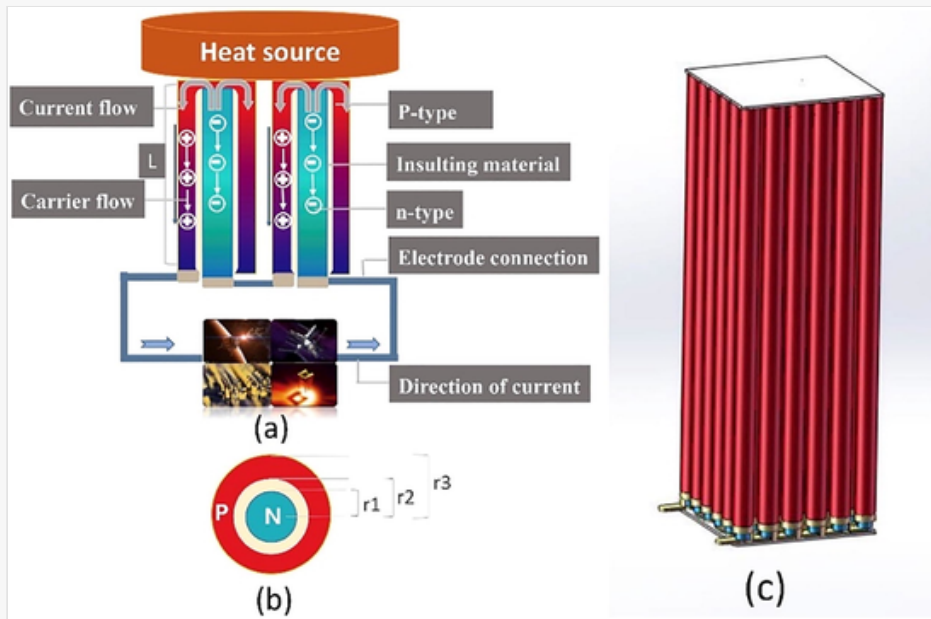
Fig. 22



Schematic of (a) fabrication process (b) simplified corrugated TEG and (c) corrugated TEG before and after thermal formation [92].

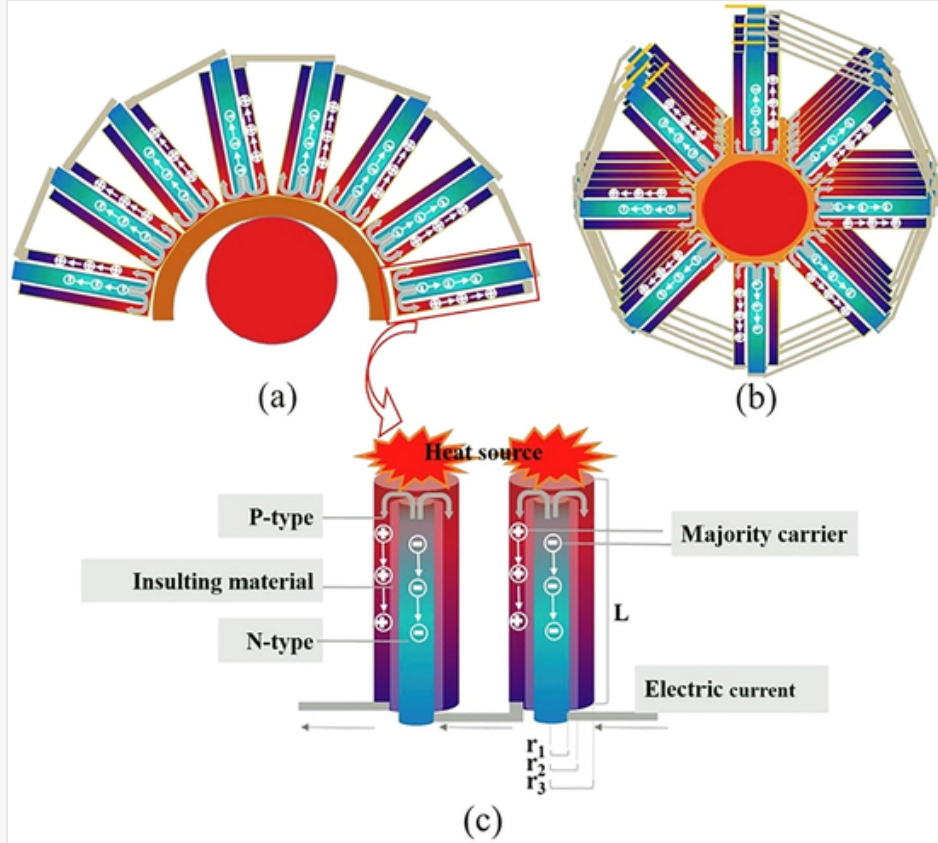
Liu et al. [93] presented the two available literatures on TEG designed with concentric filament architecture. In [93], they designed a concentric thermoelectric filament structure (shown in Fig. 23) for radioisotope TEG which could be used in aerospace microelectronic devices because of its low power and high voltage. It was found that the thermoelectric filament TEG provided an open circuit voltage which was greater than that of the TEG with traditional π -type structure by 2.4 times. In a subsequently study [94] a TEG designed based on concentric filament architecture (shown in Fig. 24) for application as a miniaturized radioisotope TEG was presented by the same authors. They found that at a 398.15 K heat source temperature, the maximum obtainable open circuit voltage and power output were 418.82 mV and 150.95 μ W respectively.

Fig. 23



(a) Concentric filament structure (b) sectional view and (c) arrayed in series [93].

Fig. 24

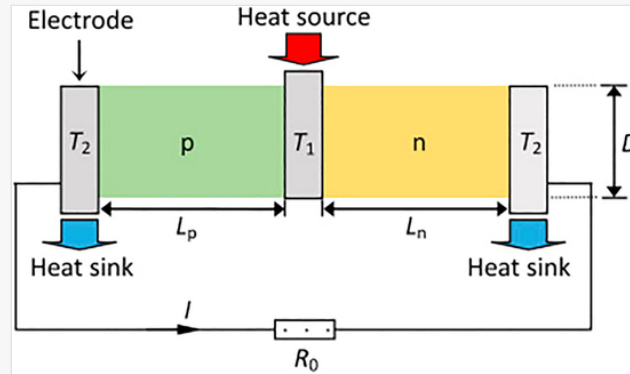


(a) Concentric filament architecture (b) sectional view and (c) monolithic construction [94].

Linear shaped thermoelectric devices have been researched by two different authors including Jia et al. [95] and Ali et al. [96]. Firstly, Jia et al. [95] presented a novel linear shaped TEG (shown in Fig. 25) which allowed the optimization of the thermoelectric legs independently because of its unique structure thus, providing better design flexibility compared to conventional π -shaped TEG. The effect of geometric parameters including leg length ratio on the linear TEG performance was studied at different total leg heights and lengths. The linear thermoelectric generator was found provide superior performance compared to the traditional π -shaped TEG and decrease of total length and/or increase of height can enhance power output [95]. In a subsequent study [97], the linear shaped thermoelectric generator transient performance was investigated by the same authors. They

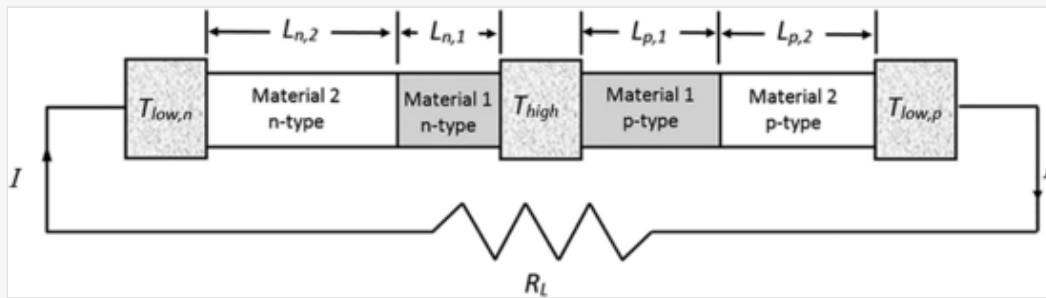
analysed how transient heat source affect the TEG performance and found that for both heating and cooling processes, the linear thermoelectric generator output power could be increased by decreasing the geometric parameter. Furthermore, Ali et al. [96] presented a new TEG design which had a pin configuration that was segmented and extended as shown in Fig. 26. It was discovered that the new design enabled the TEG to function at two different temperatures on the cold sides. In addition, it was found that the TEG performance improved because of the new design. Subsequently, the same authors presented a new design of a TEG which was made up of segmented pin configuration and tapered extended legs [98]. They found that the TEG maximum efficiency increased because of the pin geometry which was tapered and the newly designed STEG provided a greater power output compared to the traditional thermoelectric generator [98].

Fig. 25



Structure of linear TEG [95].

Fig. 26



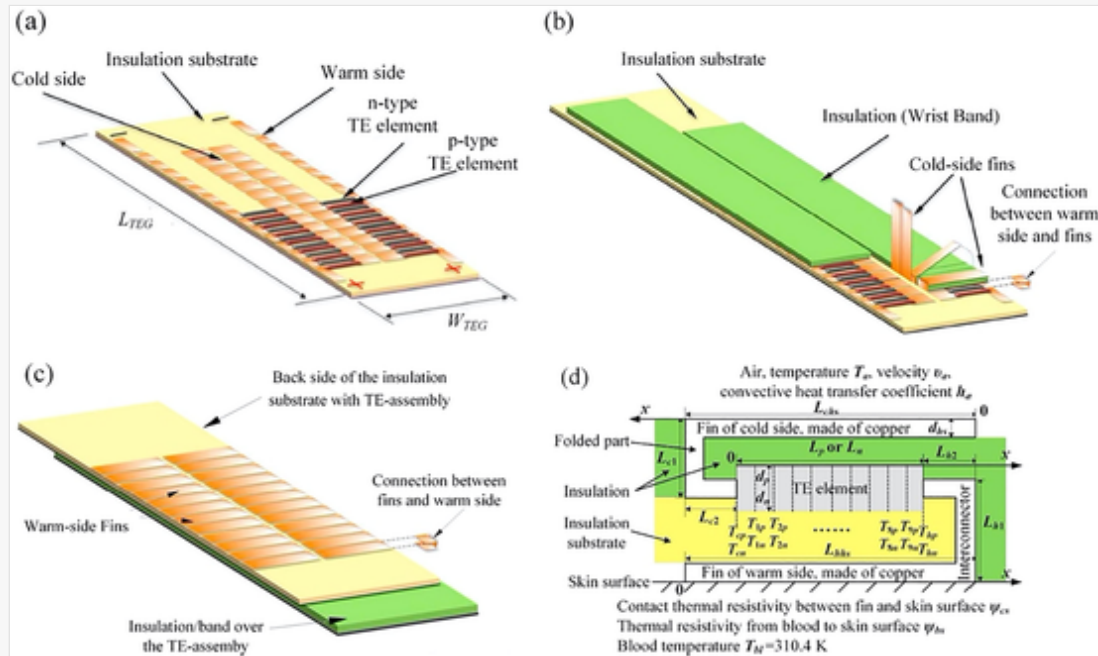
Schematic of TEG with extended and segmented pin configuration [96].

3.5.6 Flexible and micro thermoelectric

In this section, papers on flexible and micro thermoelectric devices are presented. Glatz et al. [99] used a new wafer level process for fabricating a micro TEG based on a novel polymer. The new TEG design was for non-planar surface application and they found that the increase of TE leg area could decrease the contact resistance and increase the output power. Similarly, Aranguren et al. [100] presented an optimized design for flexible polymer thermoelectric generators. The polymer TEG geometry was optimized using a validated numerical model for increased output power. Results showed that polymer TEG obtained a power output 6 times less that of a bismuth telluride TEG however, the authors argued that the polymer TEG could be advantageous for large applications. Furthermore, Qing et al. [101] presented the design of flexible TEG (shown in Fig. 27) for human body sensor. They used a steady state one-dimensional model and found that the temperature of the ambient

significantly influenced the TEG performance. Reveals also revealed that the flexible TEG could be used for powering sensors for the human body. Recently, Karthikeyan et al. [102] presented a wearable and flexible thin film thermoelectric module for multi-scale energy harvesting. They found that the new design decreased the thermal impedance and increased the temperature gradient, thereby increasing the power conversion efficiency compared to bulk thermoelectric generator.

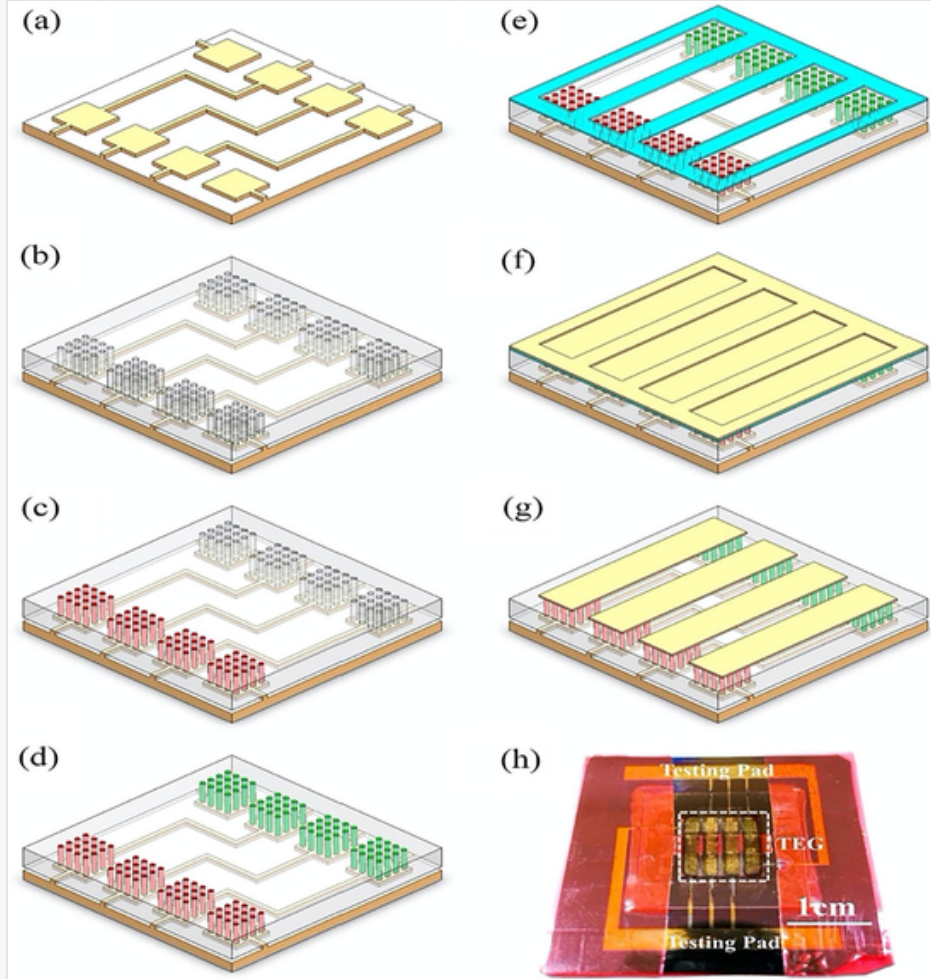
Fig. 27



Structure of two-rows flexible TEG (a) flexible substrate (b) cold-side fins (c) warm-side fins and (d) cross-sectional view [101]

Dunham et al. [103] optimized the power density of a micro thermoelectric generator. They used a closed-form solution which provided results very similar with the coupled iterative solution to model the micro TEG. Results showed that for a given fill fraction, increasing the thermoelectric legs number could help reduce the losses resulting from the electrical interconnects. In addition, the same authors experimentally studied a micro-fabricated thermoelectric generator for smart sensor and wearable applications [104]. They found that the micro TEG with 13.8 mm^2 footprint and temperature difference of 7.3 K produced a 1mW maximum output power. Furthermore, Liu et al. [105] fabricated a micro TEG (shown in Fig. 28) based on through glass pillars. The authors performed a numerical and experimental study and found that each thermocouple delivered a 10.22 mV voltage at open circuit and a large difference in temperature of 138 K was established.

Fig. 28



Fabrication process of micro TEG [105].

4 Thermoelectric geometry and structure optimization methods

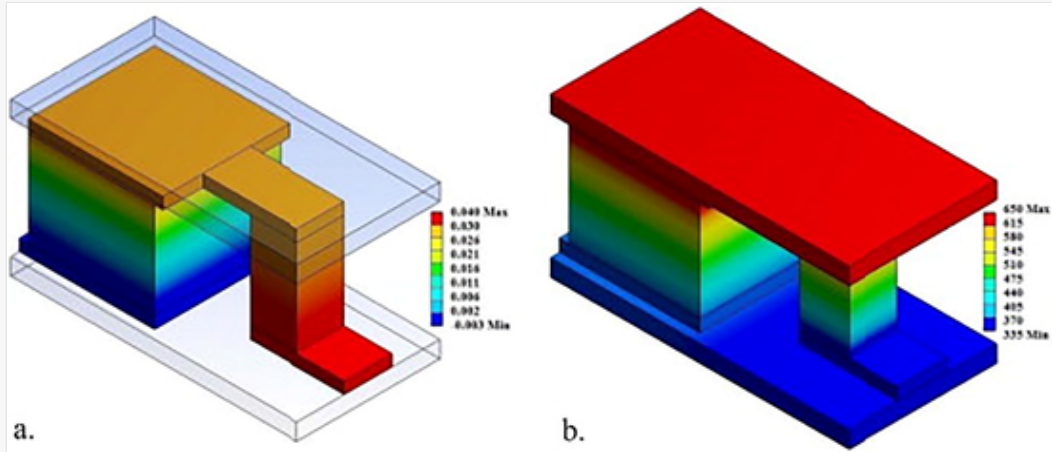
In this section, two main thermoelectric geometry and structure optimization methods for performance enhancement are discussed including three-dimensional and multi-objective methods. Furthermore, papers, which used both optimization methods, are also reviewed in this section.

4.1 Three-dimensional finite optimization

A more accurate simulation could be obtained using three-dimensional modelling which also provides a better understanding of temperature distribution and heat transfer process in systems thereby enhancing performance predictions [106]. Bjørk et al. [107] analysed thermoelectric generator heat losses internally, using a three-dimensional finite element numerical model. They found that the use of a good insulating material positioned in the middle of the TE legs could help reduce heat losses and maximize the efficiency. Rezania et al. [108] studied how thermoelectric footprint significant affected the TEG performance. Finite element method (FEM) was used

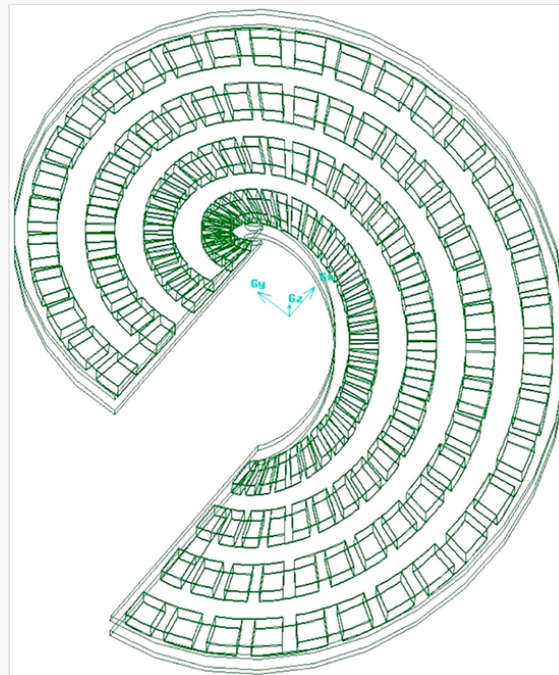
to perform the numerical study and Fig. 29 shows the voltage and temperature distributions in the uni-couple considered. Results revealed that when $A_n/A_p < 1$, maximum TEG output power and cost-performance could be obtained. Furthermore, Shi et al. [109] optimized the geometric parameters of a real-sized TEG using a three-dimensional model and FEM. Results showed that variation of the leg geometry or number of legs affected the temperature difference and temperature distribution at the hot-side simultaneously. Meng et al. [110] presented a three-dimensional numerical study of helical TE module (shown in Fig. 30) using finite volume method (FVM) and a comparison with conventional straight module was also presented. Comparing the helical module and straight module, they found that the power output of the helical module was higher and the helical TEG power output and efficiency were positively influenced by increasing the pitch.

Fig 29



(a) Voltage and (b) temperature distributions [108].

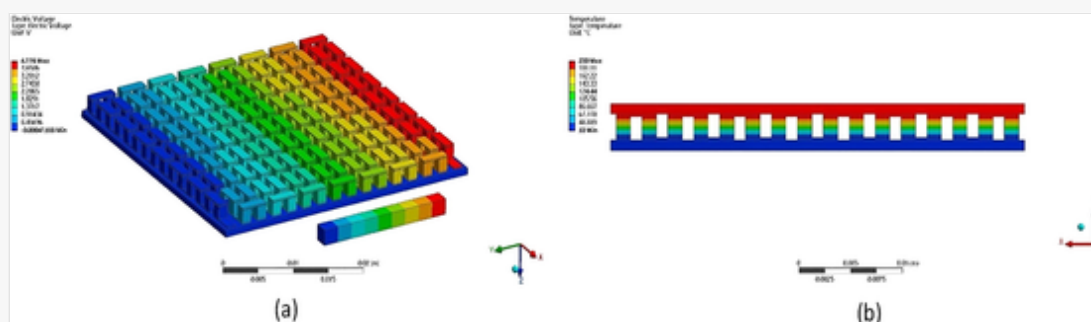
Fig. 30



Single cycle of helical TEG [110].

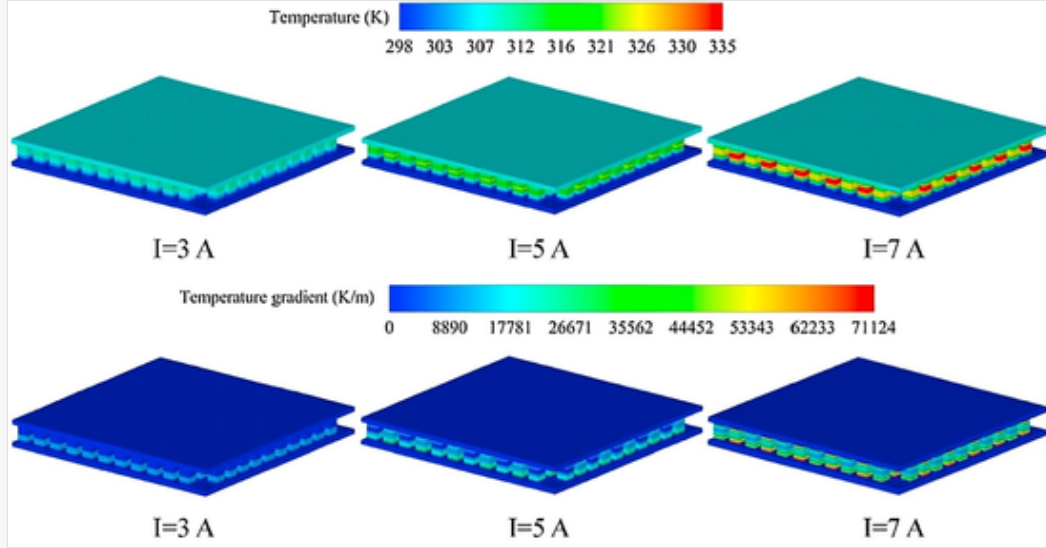
Ming et al. [111] studied a compact TEG numerically and analytically. The numerical study was conducted using ANSYS and results showed that the new compact TEG performed excellently. The authors argued that the newly designed TEG was utilized space efficiently while maximizing output power therefore, it could be applied in areas such as automobile and aerospace. Furthermore, Fernández-Yañez [112] used a 3D model to investigate a TEG thermal performance. The thermoelectric generator internal geometry and dimensions effect on system performance as well as the potential for energy recovery of the TEG were presented. The authors argued that the developed 3D computational fluid dynamics (CFD) model allowed an insight into the heat transfer process in the modules which is not experimentally possible without altering the heat transfer. Ferreira-Teixeira et al. [113] used FEM and COMSOL Multiphysics software to perform TEG geometric optimization. Cubic and cylindrical thermoelectric leg geometries were studied, and they observed an identical performance from both geometries under the same conditions. In addition, they observed an output power increase as the leg area increased and they recommended that the leg area and copper contact area should be the same for output power enhancement. Lee et al. [114] used 3D FEM to investigate the performance of a TEG and they observed a decrease in thermal resistance as the leg spacing increased. In addition, they found that the use of analytical equations and effective properties could cause the TEG performance to be accurately predicted across a wide range of operation. Liao et al. [115] presented a three-dimensional finite element model for a TEG with 127 thermocouples (shown in Fig. 31) and an experiment was performed to validate the simulation. They found that both the temperature difference and maximum output power increased by 10.2% and 14.8% respectively by the use of TEG with fins in comparison to when fins were not used. Furthermore, Wang et al. [116] optimized the geometry of a TEG and results showed that larger cross-sectional area ratio and lower leg height provided an enhanced power output. Lead telluride thermoelectric material was used, and the authors argued that optimization of thermoelectric geometry was a very good approach to achieve performance enhancement. Gong et al. [117] optimized the design of a compact TEC using a 3D FEM model. The temperature distributions in the TEC for different electric current are shown in Fig. 32 and they found that the TEC performance was significantly affected by the Joule heat. In addition, they observed an inverse relationship between the TEC coefficient of performance and cooling capacity. Thermoelectric legs with short height were also found to provide enhanced performance in terms of cooling.

Fig. 31



TEG (a) voltage and (b) temperature distributions [115].

Fig. 32



Temperature distributions (upper row) and temperature gradient contours (lower row) [117].

4.2 Multi-objective optimization

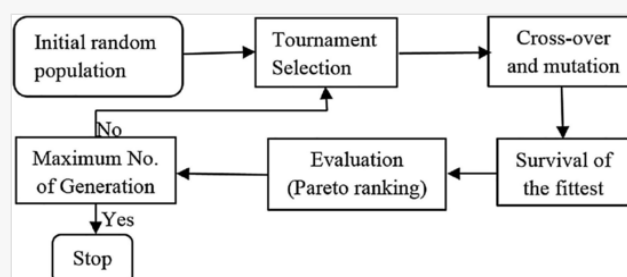
Since several parameters of a thermoelectric geometry need to be optimized concurrently to achieve optimum performance, multi-objective optimization methods have received great interests recently for thermoelectric geometry optimization. The process of optimizing two or more contrary objective functions simultaneously under specific constraints is called multi-objective optimization [118]. The three-dimensional optimization method is time consuming and might not be able to consider all possible design variables simultaneously therefore, multi-objective optimization methods provide the best and most efficient results for thermoelectric geometry optimization. Khire et al. [119] used multi-objective optimization to simultaneously minimize two design objectives and they found that to operate the thermoelectric coolers, the total input power required decreased with an increase in TEC distribution density. In addition, the authors observed that on the thermoelectric cooler, the thermal resistance of the attached heat sink significantly influenced the required number of thermoelectric coolers. Cai et al. [120] used an improved Powell algorithm along with a discrete numerical model to optimize a STEG geometry. Results revealed that the STEG performance improved due to geometry optimization. Furthermore, the authors argued that compared to genetic algorithm and particle swarm optimization algorithm, the Powell method provides a fast-ultimate convergence rate. Khanh et al. [121] performed geometry optimization of thermoelectric coolers (TECs) using simulated annealing. The dimension of TECs were optimized using simulated annealing to maximum the rate of refrigeration. The authors argued that the simulated annealing provided better optimal dimensions of the thermoelectric coolers with a larger value of rate of refrigeration compared to genetic algorithm used in a previous study [122].

Furthermore, Lossec et al. [123] used particle swarm optimization and Pareto dominance to optimize the size of a TEG. Optimization parameters such as capture surface area of the TEG, leg length, heatsink presence and height were considered, and results showed increasing the leg length of the thermoelectric generator until it reaches an optimum value allowed the performance of thermal impedance matching. In addition, the authors argued that when the electrical power value is high, the use of heatsink is imperative to ensure the thermal coupling with the environment is improved. Similarly, Ibrahim et al. [124] optimized the geometry of a thermoelectric generator for efficiency and output power enhancement using three different evolutionary algorithms. Geometric parameters

such as shape factor and leg length size were considered, and results showed that the shape factor and leg length size significantly affected the TEG performance. It was also found that thermoelectric legs which are non-parallel are better for operational conditions which are fixed because they provided enhanced TEG performance. Furthermore, Takezawa et al. [125] used topology optimization to optimize the geometry of TEG. Design parameters such as thermoelectric material type, volume, and installation position shape and temperature were considered in the optimization. Furthermore, the optimized objective functions were efficiency and output power and a sensitivity analysis for these functions was carried out. Results revealed that when only the efficiency is considered, a large percentage (>50%) of the volume could be classified as being redundant. In addition, the authors argued that in optimized thermoelectric devices which had a heating route that was simple bent, voids were not required. Similarly, Lundgaard et al. [126] used topology optimization to optimize segmented thermoelectric generators and coolers in two different studies. In [126], the off-diagonal output power and figure of merit of a STEG was optimized using density based topology optimization and they found that the design results obtained using topology optimization outperformed those obtained using analytical method by 229% and 233% for the power output and figure of merit design problems respectively. Furthermore, the same authors optimized a segmented thermoelectric cooler using density based topology optimization and found that the TEC cooling power increased by 48.7% and the TEC efficiency increased by 11.4% [127].

Genetic algorithm (GA) has been vastly used for geometry optimization in thermoelectric generators and coolers due to the large number of variables needed to be optimized [128]. Furthermore, genetic algorithm can be used to solve optimization problems that are constrained or unconstrained by using a selection method which follows the principles of biological evolution in a simplified manner [129]. Arora et al. [130] used NSGA-II to optimize a two-stage TEG. In [130], results showed that the optimization using multiple objective functions provided a more accurate solution compared to single/dual objective optimization. In a subsequent study [131], Pareto frontier was obtained for the multiple objective functions and Fig. 33 shows the NSGA-II algorithm flowchart used. Furthermore, Lamba et al. [132] used genetic algorithm to optimize the geometry of a trapezoidal shaped thermoelectric heat pump and found that the genetic algorithm population quickly converged after 20 runs, thereby proving that it is a cost effective and fast optimization tool. In addition, they found that the system heating load was negatively affected by the Thomson effect and contact resistance also reduced the performance of the system.

Fig. 33



NSGA-II algorithm flowchart [131].

4.3 Combined optimization

Three-dimensional finite difference method (FDM), finite volume method (FVM) and finite element method (FEM) have been combined with multi-objective optimization methods to accurately optimize the thermoelectric geometry for performance enhancement. Jang et al. [133] used a combination of three-dimensional FDM and

simplified conjugate-gradient method (shown in Fig. 34) to optimize the TEG spacing and spreader thickness. Results revealed that the heat transfer coefficient of the waste gas significantly influenced the optimum TEG spreader thickness and spacing. Furthermore, the authors chose the TEG power density has the objective function which was maximized, and they argued that the use of a heat spreader with the right size could cause a decrease in the thermal resistance and using a heat spreader provides a 50% power output enhancement. Similarly, Meng et al. [134] optimized a thermoelectric generator model with simplified conjugate-gradient algorithm and a model which had multiple physics. Geometric parameters of the thermoelectric generator were optimized, and the authors recommended the use of multi-objective optimization for simultaneous output power and efficiency improvement. They argued that optimizing the output power only led to an increase in output power however the efficiency decreased and vice versa. Furthermore, Liu et al. [135] used three-dimensional optimization method and simplified conjugate-gradient method (SCGM) to optimize a two-stage TEG geometry. Thermoelectric geometric parameters were optimized, and results showed that both parameters (area and length ratios) greatly affected the TEG performance. The optimal design with different objectives is shown in Table 2 including the multi-objective optimization results. In addition, COMSOL and MATLAB were used to solve the 3D model and SCGM algorithm respectively and the authors argued in favour of multi-objective optimization rather than single-objective optimization. Similarly, Huang et al. [136] optimized the geometry of TEC using simplified conjugate-gradient method and three-dimensional method. At a fixed temperature difference and current, the thermoelectric leg number, leg length and cross-sectional area were optimized simultaneously, and they found that the cooling rate of the TEC increased by 1.99–10.21 at a temperature of 20 K due to geometry optimization compared with the initial TEC geometry. In addition, they found that under conditions of small current and high temperature difference, the thermoelectric cooler cooling rate could be increased by the use of a greater number of thermoelectric legs.

Fig. 34

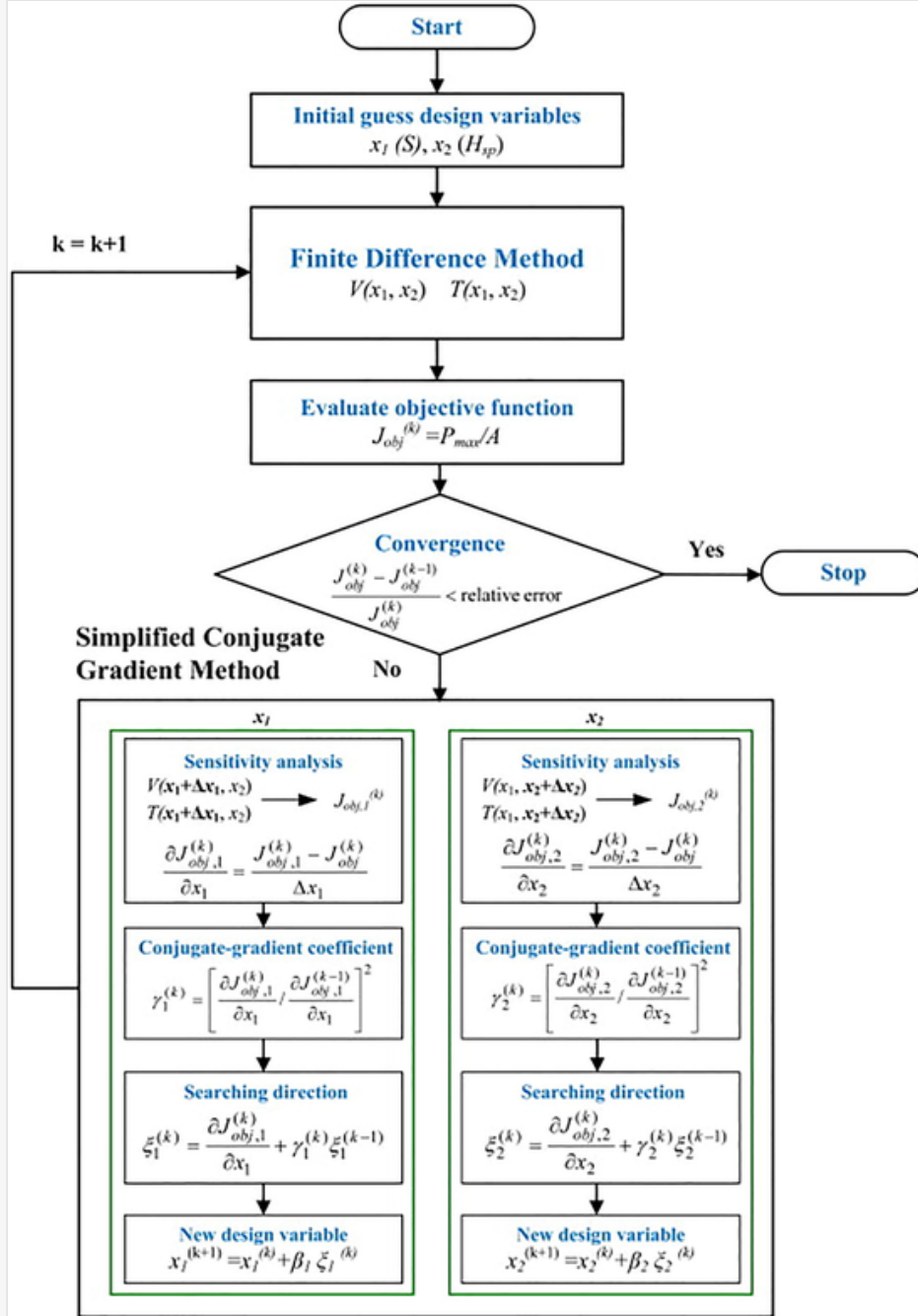


Table 2

i The table layout displayed in this section is not how it will appear in the final version. The representation below is solely purposed for providing corrections to the table. To preview the actual presentation of the table, please view the Proof.

Optimal design with different objectives [135].

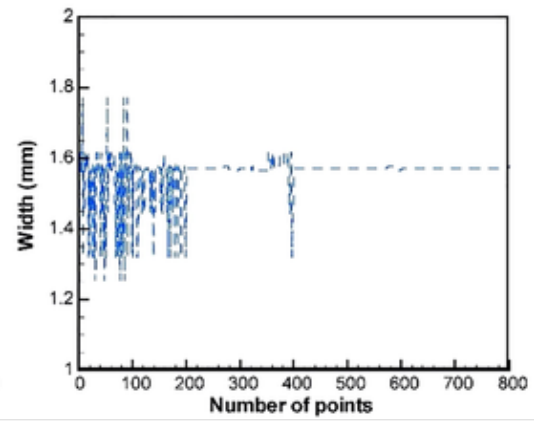
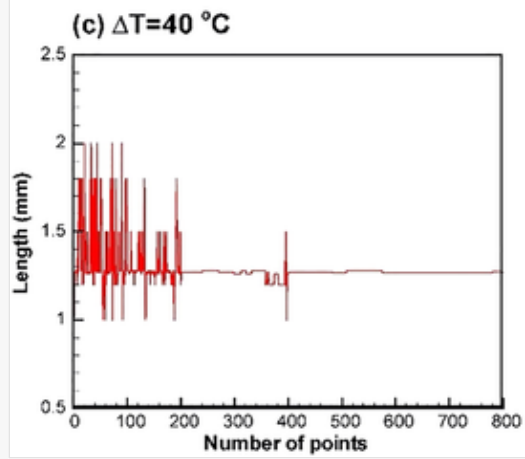
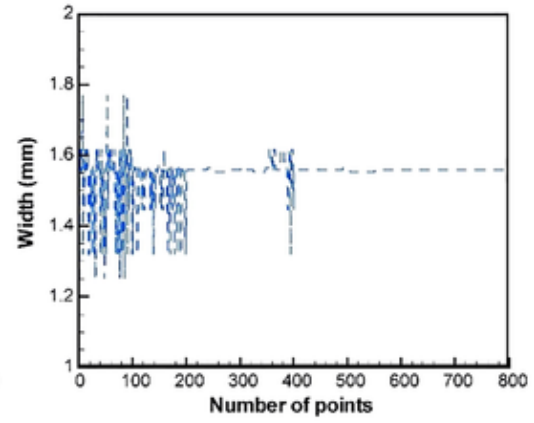
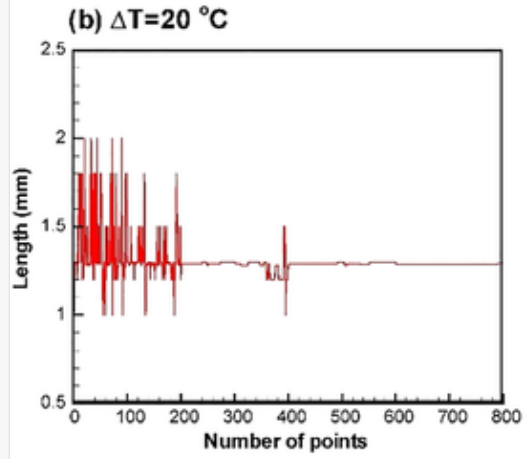
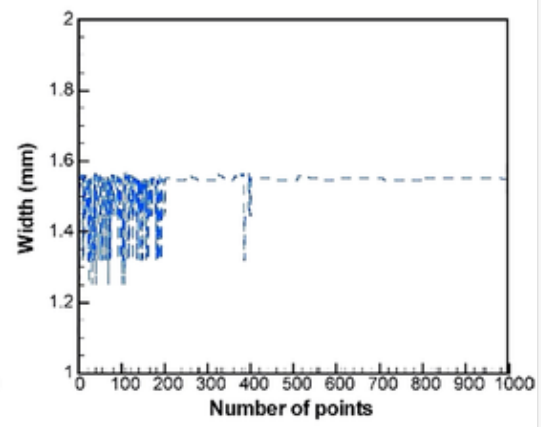
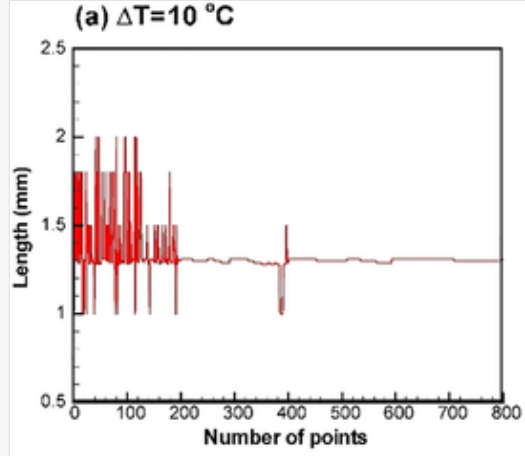
T_h (°C)	Initial design		η as objective		P as objective		Multi-objective	
	$P(W)$	η	$P(W)$	η	$P(W)$	η	$P(W)$	η
200	0.0140	0.0700	0.0149	0.0793	0.0151	0.0755	0.0150	0.0780
300	0.0337	0.1038	0.0342	0.1050	0.0355	0.1025	0.0355	0.1043
400	0.0595	0.1280	0.0605	0.1293	0.0653	0.1274	0.0651	0.1289
500	0.0871	0.1430	0.0942	0.1515	0.1038	0.1500	0.1036	0.1513
600	0.1168	0.1460	0.1332	0.1713	0.0151	0.1690	0.1506	0.1710
700	0.1440	0.1429	0.1774	0.1880	0.2064	0.1862	0.2058	0.1877

Kishore et al. [137] optimized the TEG geometry using a combination of Taguchi method and three-dimensional method. In [137], analysis of variance (ANOVA) was used alongside the Taguchi optimization method for STEG performance enhancement and results from using the Taguchi method should that the optimum cross-sectional area and total leg height for maximum power output were $2.25 \times 2.25 \text{ mm}^2$ and 3 mm respectively. While in a subsequent study [138], a non-segmented bismuth telluride TEG was optimized using Taguchi method and three-dimensional numerical method. Results revealed the optimum leg cross-sectional area and height for maximum efficiency to be $1.5 \times 1.5 \text{ mm}^2$ and 1.75 mm respectively. Similarly, Taguchi method was used to optimize TEG performance by Chen et al. [139]. The heat sink width and length, fin thickness and height were optimized, and results revealed that the heat sink length affected the heat transfer rate the most. In addition, they found that the key factor the affected the TEG efficiency and output power was the temperature of the hot side while the width of the heat sink had almost negligible effect. Soprani et al. [140] optimized the TEC performance using topology optimization and three-dimensional FEM. The experimental results and model forecasts agreed very well. The method for optimization was utilized to design electronic devices which were cooled actively and could be used as an intervention tool for downhole oil. Furthermore, within the electronic device/unit, the distribution of aluminium and material for thermal insulation were optimized using the model.

Hegmanns et al. [141] performed multi-objective TEG optimization using genetic algorithm and 3D finite element model. The aim of the optimization efforts was to reduce the mechanical stress and improve the electric power density of the thermoelectric generator under realistic boundary conditions. It was found that the use of multi-objective optimization methods for geometry optimization enabled the significant reduction of mechanical stress. Similarly, Chen et al. [142] used a combination of multi-objective genetic algorithm (MOGA) and FEM to perform geometry TEG geometry optimization. Fig. 35 shows the evolution of TEG width and length with the

algorithm process. The authors argued that to obtain better performance from the TEG through geometry optimization, MOGA is a powerful tool that can be used. Results also revealed that under a specific heat flux condition, the efficiency and power output of the TEG could be increased by increasing the thermoelectric leg length/height however, when a fixed temperature difference is used, the TEG power output increased as thermoelectric leg length decreased. Furthermore, Ge et al. [143] used a combination of MOGA and FEM to optimize STEG and results showed that to obtain increased output power from the STEG, there is an optimal leg length ratio which should be used. The thermoelectric materials used for the hot side and cold side were Skutterudite and bismuth telluride respectively. Furthermore, the authors optimized two objectives simultaneously including maximum power output and minimum volume of semiconductor. In addition, results revealed that the STEG performed better than the Skutterudite TEG. Meng et al. [144] used a combination of NSGA-II and three-dimensional FEM model to optimize a two-stage thermoelectric combined device. They found that the leg ratio between the TEG and TEC alongside that between the two stages of the thermoelectric generator and cooler has an optimum number. Furthermore, it was found that at the interface of the different stages, the accumulated heat caused the reduction in performance. Recently, Sun et al. [145] optimized a two-stage TEG [145] and a two-stage TEC [146] using finite element method and NSGA-II. It was found that there is an optimal ratio for cross-sectional area at both the lower stage and upper stage at which the power output can be maximized [145]. Similarly, they found that for the two-stage thermoelectric cooler, the ratio of TE legs between the upper and lower stages as an optimum number for obtaining maximum COP [146].

Fig. 35

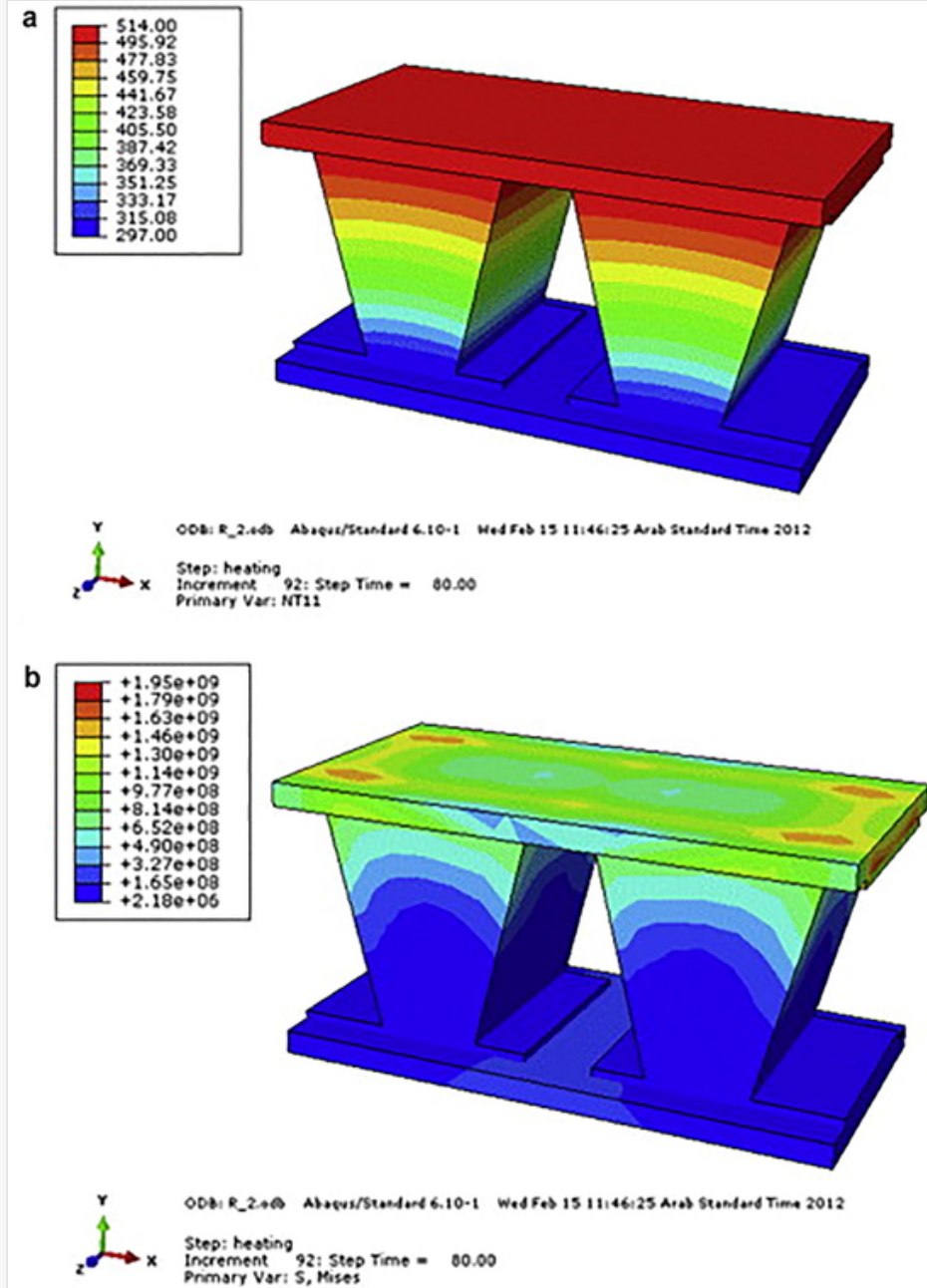


Process of parameter evolution of length and width of TEG for temperature difference of (a) 10 °C (b) 20 °C and (c) 40 °C [142].

5 Thermal stress optimization

Either in cooling/heating or power generation applications, the temperature difference in TE legs cause thermal stress due to the fact that the thermal expansion of the materials is different. Consequently, it is important to perform thermal stress analysis and optimization to provide information on locations of high stress in the legs [147]. The main aim of thermal stress optimization study is to significantly decrease the thermoelectric legs thermal stress which in turn helps to increase the thermoelectric device life span. Clin et al. [148] observed the high stress locations in the thermoelectric legs to be around the corners of the legs. Furthermore, they found that the stress at the thermoelectric leg corners could be reduced by soldering alloy plastic deformation. In addition, it was found that the distribution of stress in the thermoelectric legs was affected greatly by the boundary conditions and the mismatch of thermal expansion coefficient between the different materials in the TE module. Similarly, Turenne et al. [149] predicted the stress level in thermoelectric module components and found that the maximum stress observed on the legs were located at the corners of the module, which were further from the centre. The numerical study was performed using finite element analysis and under conditions of steady state. Furthermore, the effect of geometric parameters on the TEG thermal stress was studied by Gao et al. [150]. They found that initially, when the TE leg length increased, the shear stress and von Mises stress reduced. ANSYS simulation software was used to perform the numerical study with finite element analysis and the stress analysis was performed by considering the mechanical material properties as anisotropic. Furthermore, the effect of TE leg geometry on TEG thermal stress was investigated by Al-Merbati et al. [151]. Three different leg geometries were studied, and they found that TE geometry optimization could lower the stress developed in the thermoelectric legs greatly. The thermoelectric leg geometry shown in Fig. 36 was found to provide the lowest thermal stress in the thermoelectric legs. Furthermore, Chen et al. [152] used finite element method to study to investigate the stress developed in a bismuth telluride TEG and found that the use of elastic-plastic model provided a more accurate representation of the stress levels in the TEG compared to the linear elastic model. This is because in the elastic-plastic model, copper and solder alloy undergo plastic deformation which reduces the stress level in the TEG. In addition, Mu et al. [153] investigated how significantly, geometric dimensions affected the stress distributions in a Mg_2Si -based TEG and found that increasing the leg width and length caused an increase in the TE legs maximum first principal stress. The numerical study was carried out using a three-dimensional finite element model and ANSYS software. In addition, they found that the copper thickness had a more pronounced influence on the maximum first principle stress compared to the thickness of the ceramic and solder.

Fig. 36

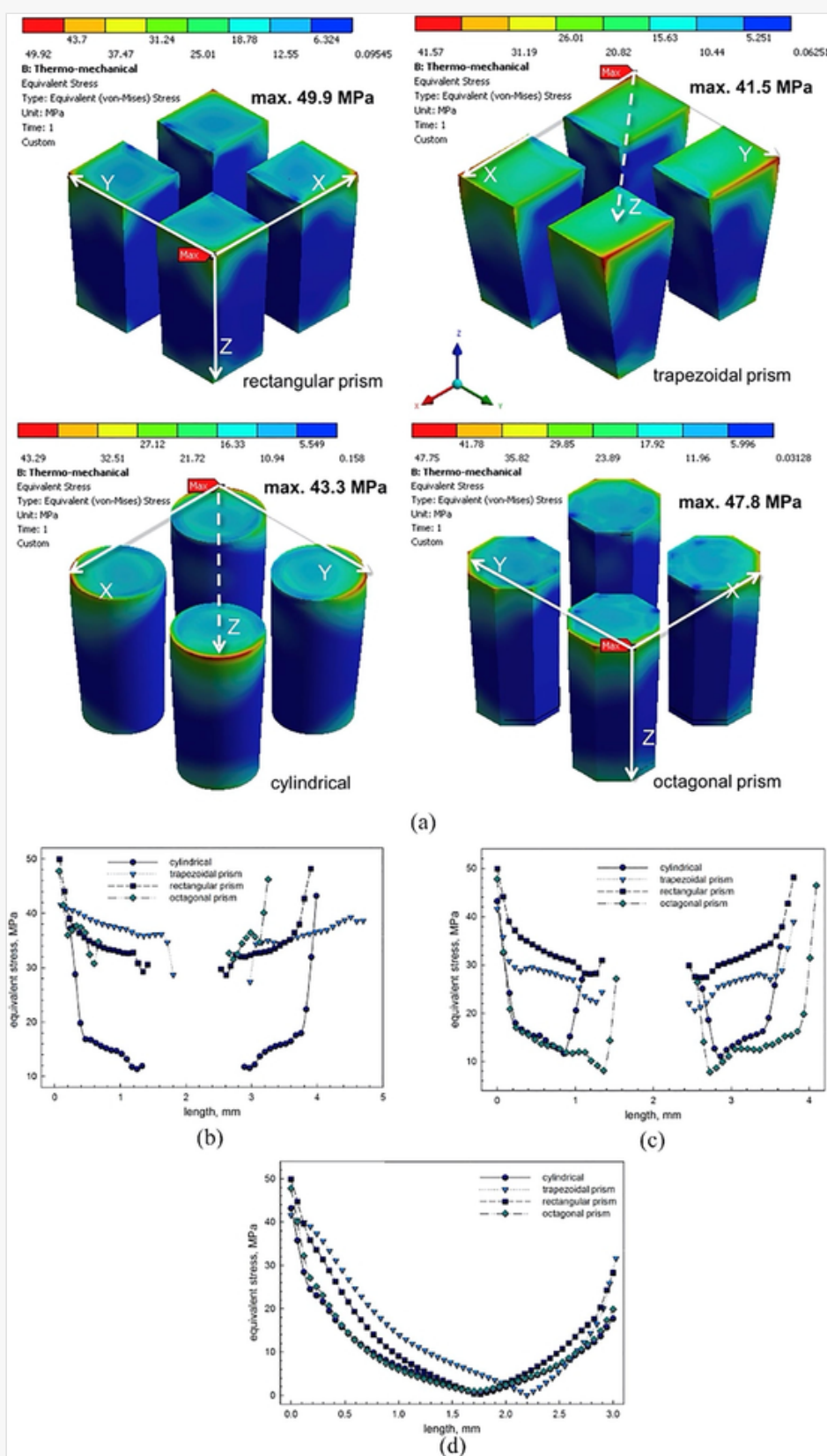


(a) 3D temperature distribution and (b) thermal stress distribution [151].

Jia et al. [154] estimated the mechanical performance of a STEG [154] and TEG [155]. The effect of segment length on the TE materials maximum stress level was studied at different temperatures and results revealed the significant decrease in STEG stress due to the deformation of solder and copper [154]. Furthermore, it was found that the maximum stress of TE legs occur on the hot end face that contact the welding strips and a reduction of thermoelectric leg length increases the maximum stress [155]. Erturun et al. [156] presented a series of studies on relationship between thermoelectric leg geometry and TEG mechanical performance. The results (shown in Fig. 37) reveal a thermal stress of 43.3 MPa in the cylindrical legs and 49.9 MPa in the rectangular legs at a temperature difference of 100 °C [156]. Furthermore, it was found that the maximum TE legs stress decreased by 10% by the use of coaxial-leg configuration [157]. In addition, the authors found that decreasing leg height, increasing leg width and spacing all led to an increase in thermal stress [158]. Ming et al. [159] studied how heat flux with a non-uniform distribution affected the stress developed in a TEG [159] and STEG [160]. Results revealed that the TEG mechanical performance was negatively impacted by the non-uniform heat flux [159]. In addition, it was found that an increase of heat concentration led to an increase in thermal stress [160]. Wu et al. [161] analysed the influence of various TE leg configurations on the developed stress in the

TEG. The effect of geometric parameters such as TE leg distance, ceramic plate thickness, copper strip thickness and soldering strip thickness on the thermal stress in a TEG was studied. Results revealed that a smaller distance between thermoelectric legs reduces thermal stress and increase TE module life expectancy.

Fig. 37

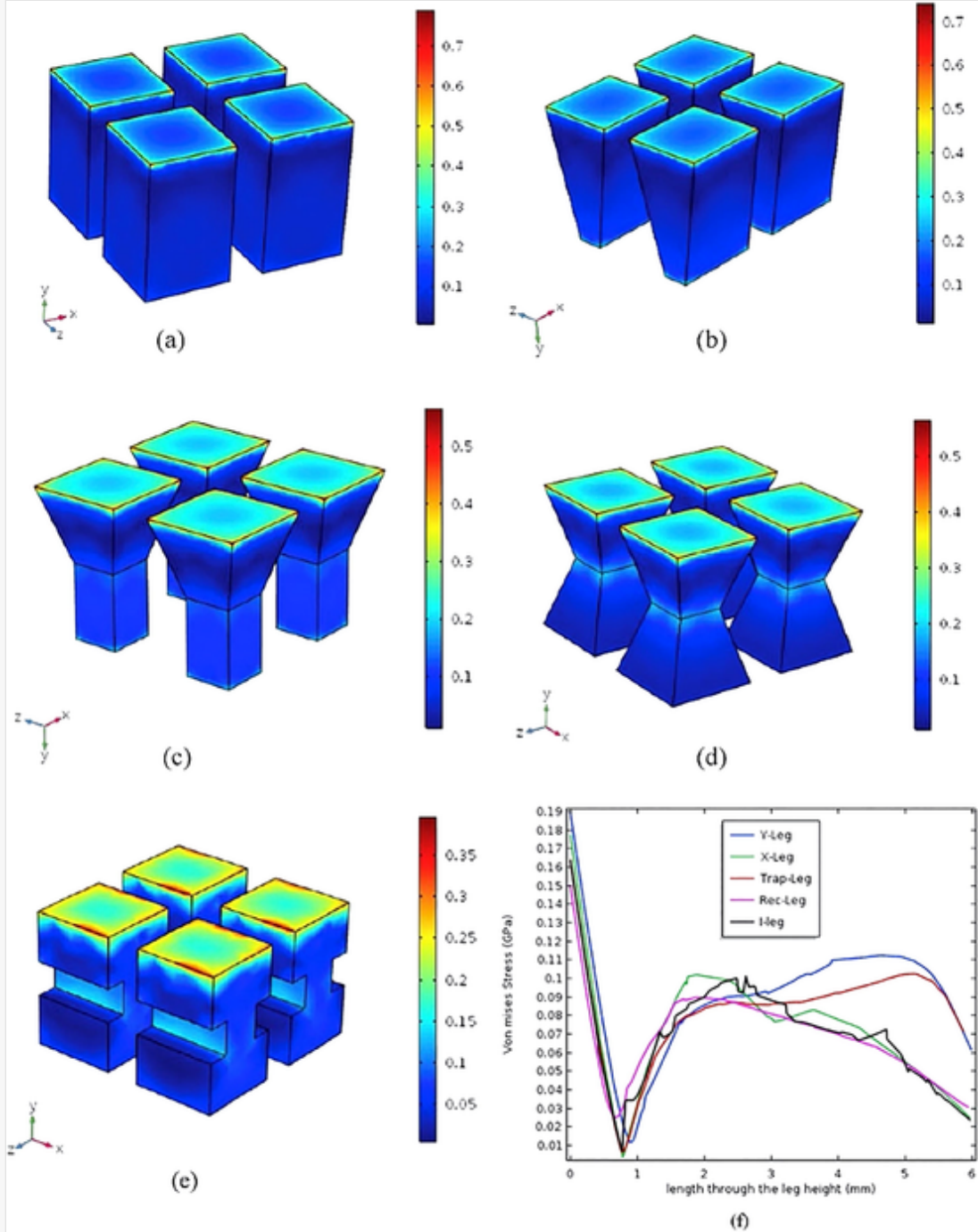


Maximum stress distribution in legs (a) as nepogram and along the (b) x-, (c) y-, and (d) z-axis paths [156].

Bakhtaryard et al. [162] performed numerical simulations for various geometries of a thermoelectric module to investigate its mechanical performance under the same operating conditions. They found that the circular

geometry provided a 13% stress decrease in comparison to that of the traditional rectangular TE geometry. Furthermore, Yilbas et al. [163] studied pin tapering effect on the stress in a TEG and they found that the regions close to interface of the hot side had high von Mises stress due to the mismatch of the ceramic and copper material properties. The thermal stress study was conducted using finite element software, ABAQUS. Karri and Mo [164] studied how significantly the geometric parameters affected the TEG thermal stress using ANSYS software and finite element analysis. Results showed the thermoelectric leg length affected the stress developed in the legs the most and the boundary conditions greatly affected the stress in the thermoelectric legs [164]. In addition, the authors argued that thermoelectric legs with long length are better for reducing thermal stress however, they also reduce the performance of the TEG [165]. Furthermore, Fan and Gao [166] studied the effect of geometric parameters on ATEG thermal stress. They found that increasing the thermoelectric leg angle ratio resulted in an initial stress decrease before it increased. In addition, results revealed the less impact of thermoelectric leg number on maximum stress in ATEG legs. It was also observed that the mechanical reliability of the ATEG could be improved by increasing the thermoelectric leg length although doing that will cause a decrease in the electrical performance of the ATEG. Ibeagwu [167] performed a comprehensive investigation on the influence of variable leg geometry on TEG stress. The authors considered four different leg geometries and they found that the thermal stress in their new geometry was lower than that in the conventional geometries as shown in Fig. 38. Furthermore, Gong et al. [168] presented two recent studies on thermoelectric cooler mechanical performance analysis using a 3D numerical model. Results revealed that attaching a thermal load to the Peltier junction would cause an extremely high thermal stress level that may in turn cause cracks and dislocations [168]. In addition, it was found that the use of transient super-cooling characteristics of the TEC could reduce thermal stress peaks [169].

Fig. 38



Thermal stress distributions in GPa for (a) Rect-leg (b) Trap-leg (c) Y-leg (d) X-leg (e) I-leg and (f) centreline stress profile [167].

6 Additional thermoelectric optimization

Asides the geometry and structure optimization of thermoelectric for performance enhancement, contact resistance optimization study is equally important. This is because, thermoelectric thermal and contact resistance are two important parameters that significantly influence the performance of thermoelectric modules [170]. Furthermore, research on heat pipe incorporation in thermoelectric systems has attracted more attention recently due to opportunity for co-generation. Heat pipes are efficient heat transfer devices [171] therefore, their incorporation into thermoelectric systems can lead to performance enhancement. The application of pulsed heating and cooling to thermoelectric generators and coolers respectively for thermoelectric device performance enhancement has been investigated more recently. Consequently, the literatures on contact resistance study, heat pipe incorporation, pulsed heating and cooling are shown in Table 3.

Table 3

i The table layout displayed in this section is not how it will appear in the final version. The representation below is solely purposed for providing corrections to the table. To preview the actual presentation of the table, please view the Proof.

Thermoelectric optimization approach for performance enhancement.

Reference	Thermoelectric device	Optimization approach	Key finding
Ebling et al. [172]	TEG	Contact resistance	Contact resistance negatively affects TEG figure of merit.
Gomez et al. [173]	TEG	Contact resistance	Electrical contact resistance can change with geometry and low electrical contact resistance is beneficial for power generation.
Fabián-Mijangos et al. [174]	TEG	Contact resistance	Parasitic contact and wiring resistances increase isothermal resistance of TEG.
Massaguer et al. [175]	TEG	Contact resistance	Thermal contact resistances significantly affect power output.
Höglblom et al. [176]	TEG	Contact resistance	Ignoring contact resistances in simulations lead to over-prediction of power output.
Luo et al. [177]	TEG	Contact resistance	Decrease of electrical contact resistance cause an increase in efficiency and effectiveness.
Ouyang et al.	TEG	Contact	Contact resistances especially the electrical one significantly affects

[178]		resistance	TEG efficiency and power output negatively.
Gupta et al. [179]	TEC	Contact resistance	Processing stacks of bulk, metal-coated TE wafers using TE industry-standard processes can be used to accurately measure contact resistance on bulk TE materials.
Pietrzyk et al. [180]	TEC	Contact resistance	Optimum B-factor did not change by more than 20% when contact resistance was varied over a range of five orders of magnitude.
Kim et al. [181]	TEC	Contact resistance	Proposed scanning probe method could accurately measure direct contact resistance.
Sun et al. [182]	TEC	Contact resistance	Thermal contact resistance negative affects performance more than electrical contact resistance.
Li et al. [183]	TEG	Heat pipe	The quantity of TEG needed and system cost can be reduced by the use of micro-channel heat pipe.
He et al. [184]	TEG	Heat pipe	Integrated solar heat-pipe/thermoelectric can be used for combined electricity generation and water heating.
Lv et al. [185]	TEG	Heat pipe	TEG can be combined with a heat pipe or collector for co-generation of electricity and hot water.
Cao et al. [186]	TEG	Heat pipe	Use of heat pipes in TEG for heat recovery can increase its popularity for automobile exhaust waste heat recovery.
Li et al. [187]	TEG	Heat pipe	A high thermal performance in addition to extra electricity generation was observed from the new system with heat pipe.
Wu et al. [188]	TEG	Heat pipe	Gravitational flat-plate heat pipe was advantageous compared to metal plate in temperature uniformity.
Asaadi et al. [189]	TEG	Pulsed heating	Rectangular pulsed heat provides best performance and transient pulsed heating enhanced performance of ATEG compared to steady state heating.
Yamashita et al. [190]	TEG	Pulsed heating	Application of periodically alternating temperature gradient improves efficiency of TEG.
Yazdanshenas et al. [191]	TEG	Pulsed heating	Range of power oscillation reduced as frequency of imposed heat flux increased.
Ruiz-Ortega et al. [192]	TEG	Pulsed heating	Temperature decrease across thermoelectric leg was more significantly when three pulses were applied.
Abdallah et al. [193]	TEG	Pulsed heating	Maximum TEG performance enhancement was achieved for a time period of 1000 s and a duty cycle of 10%.
Yan et al. [194]	TEG	Pulsed heating	Figure of merit and TEG conversion efficiency can be improved by the use of sinusoidal or square-wave periodic temperature gradient.
Chen et al. [195]	TEG	Pulsed heating	To obtain enhanced efficiency, pulsed heat power is better than alternating temperature gradient.
Synder et al. [196]	TEC	Pulsed cooling	Thermoelectric figure of merit is the key material parameter for pulse cooling.
Thonhauser et al. [197]	TEC	Pulsed cooling	Supercooling effect could be improved using quadratic pulse form and a maximum temperature decrease of 116 K was obtained.

Chakraborty et al. [198]	TEC	Pulsed cooling	Process paths of pulsed and non-pulsed operations of TEC were accurately mapped.
Shen et al. [199]	TEC	Pulsed cooling	When the magnitude of the pulse is smaller than the optimal pulse magnitude, voltage pulse can effectively reduce transient cold side temperature.
Ma et al. [200]	TEC	Pulsed cooling	Periodic supercooling effect could be achieved by properly designing the current period.

7 Future research direction

Thermoelectric geometry and structure optimization are hot research fields currently being paid a lot of attention due to the huge potential for performance enhancement of thermoelectric generators and coolers. Regarding the optimization of thermoelectric leg length or height, it has been reported that the thermoelectric generator efficiency and power output have a linear and inverse relationship respectively, with the thermoelectric leg length. Furthermore, the optimum leg length ratios for maximum efficiency and output power in a segmented thermoelectric generator have been reported to be different. Therefore, optimizing the thermoelectric leg length for linear enhancement of power output and efficiency of TEG and STEG is a main issue which should be paid more attention in future. Furthermore, attention should be paid to the heat source condition used for a thermoelectric generator when leg length optimization is performed. This is because of the result reported which states that the optimum leg length for maximum power output under constant heat flux and constant temperature conditions are different. Consequently, leg length optimization is recommended whenever heat source condition is changed. While the efficiency of a thermoelectric generator increases as the leg length increases, the hybrid photovoltaic-thermoelectric system efficiency decreases as the leg length increases. In addition, it was reported that the optimum leg cross-sectional area in a thermoelectric generator and hybrid photovoltaic-thermoelectric system is different. This difference is due to the presence of the photovoltaic in the hybrid system which contributes the greater percentage of the hybrid system efficiency and power output. Consequently, it is recommended to perform leg length and leg cross-sectional area optimization in both a thermoelectric only device and a hybrid system as the results might be different.

Since the thermoelectric legs are connected electrically in series, the output voltage and power of the thermoelectric generator could be increased by increasing the number of thermoelectric legs. However, it was reported that reducing the leg number could enhance the power output of a solar thermoelectric generator under non-uniform solar illumination. Consequently, it is recommended that this phenomenon be studied more in detail and optimum leg number for solar thermoelectric generators under uniform and non-uniform illumination be investigated. Furthermore, asymmetrical thermoelectric legs have been reported to provide enhanced performance compared to the conventional rectangular/symmetrical legs due to the better heat transfer in the asymmetrical legs. However, currently only one experimental paper on asymmetrical thermoelectric legs is available in literature. Therefore, to increase the chances of commercialization of TEG and TEC with asymmetrical legs, more experimental studies alongside numerical optimization needs to be performed and are thus, recommended. In addition, more studies on the combined effects of thermoelectric leg length, area, number and shape on thermal stress in a thermoelectric generator and cooler are recommended.

Geometry mismatch can be eliminated by the use of annular thermoelectric generators and coolers when round shaped heat sources and sinks are used. Consequently, more attention is being paid recently to annular TEG and TEC however, the current available studies have considered only annular uni-couples. Therefore, more research

on full-scale optimization of annular thermoelectric generators and coolers are recommended to facilitate wider adoption. Furthermore, segmentation of thermoelectric materials is an effective method to enhance performance by combining highly efficient materials at specific temperature ranges. However, the thermoelectric materials must be carefully selected to ensure they are compatible. In addition, the segmented geometry must be optimized for performance enhancement. Consequently, more research on geometry optimization in segmented thermoelectric devices is recommended. Furthermore, cascaded thermoelectric devices can be connected electrically in series, parallel or separately. Therefore, geometry optimization of cascaded thermoelectric generators and coolers under each of these electrical connection methods is recommended as the results might be different. Research on flexible and micro thermoelectric devices is recommended in order to facilitate the wider use of thermoelectric devices in wearable devices and micro energy harvesting.

Three-dimensional finite optimization studies are very important as they provide more information about temperature distribution in TEG and TEC as well as providing more accurate results close to real values. More three-dimensional parametric studies are encouraged for optimizing the TE geometry for the different geometry and structure types. Multi-objective optimization has been shown to be an efficient method to perform comprehensive and simultaneous optimization of various thermoelectric geometry parameters. The combination of three-dimensional finite optimization and multi-objective optimization is very important and significant as it combines the advantages of each of the individual optimization methods. Three-dimensional finite element/volume method can provide detailed thermal stress distributions to locate the positions of high stress while multi-objective optimization can efficiently optimize the thermoelectric geometry while considering both the electrical and mechanical performance of the device. Therefore, research on combined three-dimensional and multi-objective optimization of TEG and TEC geometry for electrical and mechanical performance enhancement is recommended as a future research direction.

Furthermore, the main drawback of all the interesting research being carried out on thermoelectric geometry optimization is the lack of experimental results to validate the numerical results and performance enhancement being predicted. There are few to none experimental research available on effect of thermoelectric geometry on electrical and mechanical reliability of TEG and TEC. Therefore, a major future research direction is experimental investigation of various thermoelectric geometries for electrical and mechanical performance enhancement. Combining the three-dimensional finite optimization and multi-objective optimization with experimental study will provide very significant insights on efficient design of thermoelectric generators and coolers.

8 Conclusion

Optimization of thermoelectric generator and cooler is a key research objective to increase their conversion efficiency. The low efficiency of thermoelectric devices alongside high material cost has hindered widespread application of thermoelectric technology despite the advantages offered by thermoelectric devices. Consequently, extensive research is being undertaken on geometry and material optimization for thermoelectric generator and cooler performance enhancement. This review presented an in-depth analysis of thermoelectric geometry and structure optimization. The main significance of geometry and structure optimization is that quantity of material needed for optimum performance could be reduced thereby providing a dual function of increasing efficiency and reducing material cost. The four main parameters including leg length or height, cross-sectional area, number of legs and leg shape which are paid attention to during optimization of thermoelectric geometry were discussed in detail. In addition, a review of the different thermoelectric structure currently available was provided including flat plate, annular, segmented, cascaded, corrugated, concentric, linear, flexible and micro thermoelectric

generators and coolers. The significant results obtained from each of these geometries and structures were presented and discussed. Furthermore, the two main optimization methods for thermoelectric geometry optimization were discussed including three-dimensional finite optimization and multi-objective optimization. In addition, papers that used both methods were also reviewed and different algorithms such as improved Powell algorithm, particle swarm optimization algorithm, simulated annealing, genetic algorithm including non-dominated sorting genetic-algorithm-II, simplified conjugate-gradient method, Taguchi method and Topology optimization were discussed in detail. An in-depth review of thermal stress optimization studies was presented and effect of thermal stress on mechanical reliability of thermoelectric generators and coolers was discussed. Furthermore, three additional thermoelectric optimization methods including contact resistance optimization, heat pipe incorporation, pulsed heating and cooling were discussed. Finally, future research directions were presented to provide valuable guidance for future research on geometry and structure optimization of thermoelectric devices.

Declaration of Competing Interest

The authors declare that they have no known competing financial interests or personal relationships that could have appeared to influence the work reported in this paper.

Acknowledgment

This study was sponsored by the Project of Marie Curie International incoming Fellowships Program (745614).

References

 The corrections made in this section will be reviewed and approved by a journal production editor. The newly added/removed references and its citations will be reordered and rearranged by the production team.

- [1] He W., Zhang G., Zhang X., Ji J., Li G., Zhao X. Recent development and application of thermoelectric generator and cooler. *Appl Energy* 2015;143:1–25. doi:10.1016/j.apenergy.2014.12.075.
- [2] Twaha S., Zhu J., Yan Y., Li B. A comprehensive review of thermoelectric technology: materials, applications, modelling and performance improvement. *Renew Sustain Energy Rev* 2016;65:698–726. doi:10.1016/j.rser.2016.07.034.
- [3] Zheng X.F., Liu C.X., Yan Y.Y., Wang Q. A review of thermoelectrics research - Recent developments and potentials for sustainable and renewable energy applications. *Renew Sustain Energy Rev* 2014;32:486–503. doi:10.1016/j.rser.2013.12.053.
- [4] Li G., Zhou K., Song Z., Zhao X., Ji J. Inconsistent phenomenon of thermoelectric load resistance for photovoltaic–thermoelectric module. *Energy Convers Manag* 2018;161:155–161. doi:10.1016/j.enconman.2018.01.079.
- [5] Li G., Shittu S., Zhao X., Ma X., Zhou K., Zhao X., et al. Preliminary experiment on a novel photovoltaic-thermoelectric system in summer. *Energy* 2019;188:116041. doi:10.1016/j.energy.2019.116041.

- [6] Lee S., Bock J.A., Trolier-McKinstry S., Randall C.A. Ferroelectric-thermoelectricity and Mott transition of ferroelectric oxides with high electronic conductivity. *J Eur Ceram Soc* 2012;32:3971–3988. doi:10.1016/j.jeurceramsoc.2012.06.007.
- [7] Elsheikh M.H., Shnawah D.A., Sabri M.F.M., Said S.B.M., Hassan H.M., Bashir A.M.B., et al. A review on thermoelectric renewable energy: principle parameters that affect their performance. *Renew Sustain Energy Rev* 2014;30:337–355. doi:10.1016/j.rser.2013.10.027.
- [8] Minnich A.J., Dresselhaus M.S., Ren Z.F., Chen G. Bulk nanostructured thermoelectric materials: current research and future prospects. *Energy Environ Sci* 2009;2:466–479. doi:10.1039/b822664b.
- [9] Shittu S., Li G., Xuan Q., Xiao X., Zhao X., Ma X. Transient and non-uniform heat flux effect on solar thermoelectric generator with phase change material. *Appl Therm Eng* 2020;173:115206. doi:10.1016/j.applthermaleng.2020.115206.
- [10] Shittu S., Li G., Akhlaghi Y.G., Ma X., Zhao X., Ayodele E. Advancements in thermoelectric generators for enhanced hybrid photovoltaic system performance. *Renew Sustain Energy Rev* 2019;109:24–54. doi:10.1016/j.rser.2019.04.023.
- [11] Li G., Shittu S., Diallo T.M.O., Yu M., Zhao X., Ji J. A review of solar photovoltaic-thermoelectric hybrid system for electricity generation. *Energy* 2018;158:41–58. doi:10.1016/j.energy.2018.06.021.
- [12] Beretta D., Neophytou N., Hodges J.M., Kanatzidis M.G., Narducci D., Martin-Gonzalez M., et al. Thermoelectrics: From history, a window to the future. *Mater Sci Eng R Rep* 2018. doi:10.1016/j.mser.2018.09.001.
- [13] Du Y., Xu J., Paul B., Eklund P. Flexible thermoelectric materials and devices. *Appl Mater Today* 2018;12:366–388. doi:10.1016/j.apmt.2018.07.004.
- [14] Yang J. Potential applications of thermoelectric waste heat recovery in the automotive industry. *Int Conf Thermoelectr ICT, Proc* 2005;2005:155–159. doi:10.1109/ICT.2005.1519911.
- [15] Amatya R., Ram R.J. Solar thermoelectric generator for micropower applications. *J Electron Mater* 2010;39:1735–1740. doi:10.1007/s11664-010-1190-8.
- [16] Francioso L., De Pascali C., Farella I., Martucci C., Cretì P., Siciliano P., et al. Flexible thermoelectric generator for wearable biometric sensors. *Proc IEEE Sensors* 2010;196:747–750. doi:10.1109/ICSENS.2010.5690757.
- [17] Pichanusakorn P., Bandaru P. Nanostructured thermoelectrics. *Mater Sci Eng R Rep* 2010;67:19–63. doi:10.1016/j.mser.2009.10.001.
- [18] Kumar Babu, Subramanian Bandla, Thakor Ramakrishna, et al. The design of a thermoelectric generator and its medical applications. *Designs* 2019;3:22. doi:10.3390/designs3020022.
- [19] Riffat S.B., Ma X. Thermoelectrics: a review of present and potential applications. *Appl Therm Eng* 2003;23:913–935. doi:10.1016/S1359-4311(03)00012-7.

- [20] Pettes A.M., Hodes M.S., Goodson K.E. Optimized thermoelectric refrigeration in the presence of thermal boundary resistance. *IEEE Trans Adv Packag* 2009;32:423–430. doi:10.1109/TADVP.2008.924221.
- [21] Champier D. Thermoelectric generators: a review of applications. *Energy Convers Manag* 2017;140:167–181. doi:10.1016/j.enconman.2017.02.070.
- [22] Ando Junior O.H., Maran A.L.O., Henao N.C. A review of the development and applications of thermoelectric microgenerators for energy harvesting. *Renew Sustain Energy Rev* 2018;91:376–393. doi:10.1016/j.rser.2018.03.052.
- [23] Rowe D.M. *Thermoelectric Handbook: Macro to Nano*. CRC Press, Taylor & Francis Group; 2006.
- [24] Min G., Rowe D.M. Optimisation of thermoelectric module geometry for “waste heat” electric power generation. *J Power Sources* 1992;38:253–259. doi:10.1016/0378-7753(92)80114-Q.
- [25] Kumar S., Heister S.D., Xu X., Salvador J.R. Optimization of thermoelectric components for automobile waste heat recovery systems. *J Electron Mater* 2015;44:3627–3636. doi:10.1007/s11664-015-3912-4.
- [26] Tian H., Sun X., Jia Q., Liang X., Shu G., Wang X. Comparison and parameter optimization of a segmented thermoelectric generator by using the high temperature exhaust of a diesel engine. *Energy* 2015;84:121–130. doi:10.1016/j.energy.2015.02.063.
- [27] Zhang G., Fan L., Niu Z., Jiao K., Diao H., Du Q., et al. A comprehensive design method for segmented thermoelectric generator. *Energy Convers Manag* 2015;106:510–519. doi:10.1016/j.enconman.2015.09.068.
- [28] Ma X., Shu G., Tian H., Xu W., Chen T. Performance assessment of engine exhaust-based segmented thermoelectric generators by length ratio optimization. *Appl Energy* 2019;248:614–625. doi:10.1016/j.apenergy.2019.04.103.
- [29] Shen L., Zhang W., Liu G., Tu Z., Lu Q., Chen H., et al. Performance enhancement investigation of thermoelectric cooler with segmented configuration. *Appl Therm Eng* 2020;168:114852. doi:10.1016/j.applthermaleng.2019.114852.
- [30] Shen Z.G., Wu S.Y., Xiao L. Assessment of the performance of annular thermoelectric couples under constant heat flux condition. *Energy Convers Manag* 2017;150:704–713. doi:10.1016/j.enconman.2017.08.058.
- [31] Zhang A.B., Wang B.L., Pang D.D., He L.W., Lou J., Wang J., et al. Effects of interface layers on the performance of annular thermoelectric generators. *Energy* 2018;147:612–620. doi:10.1016/j.energy.2018.01.098.
- [32] Shen Z.-G.G., Liu X., Chen S., Wu S.Y., Xiao L., Chen Z.-X.X. Theoretical analysis on a segmented annular thermoelectric generator. *Energy* 2018;157:297–313. doi:10.1016/j.energy.2018.05.163.
- [33]

Shittu S., Li G., Zhao X., Ma X., Akhlaghi Y.G., Ayodele E. High performance and thermal stress analysis of a segmented annular thermoelectric generator. *Energy Convers Manag* 2019;184:180–193. doi:10.1016/j.enconman.2019.01.064.

- [34] Fan S., Gao Y. Numerical analysis on the segmented annular thermoelectric generator for waste heat recovery. *Energy* 2019;183:35–47. doi:10.1016/j.energy.2019.06.103.
- [35] Asaadi S., Khalilarya S., Jafarmadar S. A thermodynamic and exergoeconomic numerical study of two-stage annular thermoelectric generator. *Appl Therm Eng* 2019;156:371–381. doi:10.1016/j.applthermaleng.2019.04.058.
- [36] Shittu S., Li G., Zhao X., Ma X., Akhlaghi Y.G., Fan Y. Comprehensive study and optimization of concentrated photovoltaic-thermoelectric considering all contact resistances. *Energy Convers Manag* 2020;205:112422. doi:10.1016/j.enconman.2019.112422.
- [37] Hashim H., Bompfrey J.J., Min G. Model for geometry optimisation of thermoelectric devices in a hybrid PV/TE system. *Renew Energy* 2016;87:458–463. doi:10.1016/j.renene.2015.10.029.
- [38] Lamba R., Kaushik S.C. Solar driven concentrated photovoltaic-thermoelectric hybrid system: numerical analysis and optimization. *Energy Convers Manag* 2018;170:34–49. doi:10.1016/j.enconman.2018.05.048.
- [39] Li G., Shittu S., Ma X., Zhao X. Comparative analysis of thermoelectric elements optimum geometry between Photovoltaic-thermoelectric and solar thermoelectric. *Energy* 2019;171:599–610. doi:10.1016/j.energy.2019.01.057.
- [40] Mahmoudinezhad S., Atouei S.A., Cotfas P.A., Cotfas D.T., Rosendahl L.A., Rezanian A. Experimental and numerical study on the transient behavior of multi-junction solar cell-thermoelectric generator hybrid system. *Energy Convers Manag* 2019;184:448–455. doi:10.1016/j.enconman.2019.01.081.
- [41] Cui Y.J., Wang B.L., Li J.E., Wang K.F. Performance evaluation and lifetime prediction of a segmented photovoltaic-thermoelectric hybrid system. *Energy Convers Manag* 2020;211. doi:10.1016/j.enconman.2020.112744.
- [42] Lavric E.D. Sensitivity analysis of thermoelectric module performance with respect to geometry. *Chem Eng Trans* 2010;21:133–138. doi:10.3303/CET1021023.
- [43] Cheng F., Hong Y., Li W., Guo X., Zhang H., Fu F., et al. A thermoelectric generator for scavenging gas-heat: from module optimization to prototype test. *Energy* 2017;121:545–560. doi:10.1016/j.energy.2017.01.025.
- [44] Fan L., Zhang G., Wang R., Jiao K. A comprehensive and time-efficient model for determination of thermoelectric generator length and cross-section area. *Energy Convers Manag* 2016;122:85–94. doi:10.1016/j.enconman.2016.05.064.
- [45] He H., Wu Y., Liu W., Rong M., Fang Z., Tang X. Comprehensive modeling for geometric optimization of a thermoelectric generator module. *Energy Convers Manag* 2019;183:645–659. doi:10.1016/j.enconman.2018.12.087.

- [46] Zhang A.B., Wang B.L., Pang D.D., Chen J.B., Wang J., Du J.K. Influence of leg geometry configuration and contact resistance on the performance of annular thermoelectric generators. *Energy Convers Manag* 2018;166:337–342. doi:10.1016/j.enconman.2018.04.042.
- [47] Cui Y.J., Wang B.L., Wang K.F., Zheng L. Power output evaluation of a porous annular thermoelectric generator for waste heat harvesting. *Int J Heat Mass Transf* 2019;137:979–989. doi:10.1016/j.ijheatmasstransfer.2019.03.157.
- [48] Nemati A., Nami H., Yari M., Ranjbar F. Effect of geometry and applied currents on the exergy and exergoeconomic performance of a two-stage cascaded thermoelectric cooler. *Int J Refrig* 2018;85:1–12. doi:10.1016/j.ijrefrig.2017.09.006.
- [49] Shittu S., Li G., Zhao X., Ma X. Series of detail comparison and optimization of thermoelectric element geometry considering the PV effect. *Renew Energy* 2019;130:930–942. doi:10.1016/j.renene.2018.07.002.
- [50] Li G., Zhao X., Jin Y.Y., Chen X., Ji J., Shittu S. Performance analysis and discussion on the thermoelectric element footprint for PV–TE maximum power generation. *J Electron Mater* 2018;47:5344–5351. doi:10.1007/s11664-018-6421-4.
- [51] Li G., Chen X., Jin Y. Analysis of the primary constraint conditions of an efficient photovoltaic-thermoelectric hybrid system. *Energies* 2017;10:1–12. doi:10.3390/en10010020.
- [52] Dongxu J., Zhongbao W., Pou J., Mazzoni S., Rajoo S., Romagnoli A. Geometry optimization of thermoelectric modules: simulation and experimental study. *Energy Convers Manag* 2019;195:236–243. doi:10.1016/j.enconman.2019.05.003.
- [53] Hodes M. Optimal pellet geometries for thermoelectric power generation. *IEEE Trans Components Packag Technol* 2010;33:307–318. doi:10.1109/TCAPT.2009.2039934.
- [54] Liang X., Sun X., Tian H., Shu G., Wang Y., Wang X. Comparison and parameter optimization of a two-stage thermoelectric generator using high temperature exhaust of internal combustion engine. *Appl Energy* 2014;130:190–199. doi:10.1016/j.apenergy.2014.05.048.
- [55] Wang X.D., Wang Q.H., Xu J.L. Performance analysis of two-stage TECs (thermoelectric coolers) using a three-dimensional heat-electricity coupled model. *Energy* 2014;65:419–429. doi:10.1016/j.energy.2013.10.047.
- [56] Yin E., Li Q., Xuan Y. Effect of non-uniform illumination on performance of solar thermoelectric generators. *Front Energy* 2018;12:1–10. doi:10.1007/s11708-018-0533-7.
- [57] Luo D., Wang R., Yu W., Zhou W. Parametric study of a thermoelectric module used for both power generation and cooling. *Renew Energy* 2020;154:542–552. doi:10.1016/j.renene.2020.03.045.
- [58] Miao Z., Meng X., Zhou S., Zhu M. Thermo-mechanical analysis on thermoelectric legs arrangement of thermoelectric modules. *Renew Energy* 2020;147:2272–2278. doi:10.1016/j.renene.2019.10.016.
- [59]

Lakeh H.K., Kaatuzian H., Hosseini R. A parametrical study on photo-electro-thermal performance of an integrated thermoelectric-photovoltaic cell. *Renew Energy* 2019;138:542–550. doi:10.1016/J.RENENE.2019.01.094.

- [60] Sahin A.Z., Yilbas B.S. The thermoelement as thermoelectric power generator: effect of leg geometry on the efficiency and power generation. *Energy Convers Manag* 2013;65:26–32. doi:10.1016/j.enconman.2012.07.020.
- [61] Ali H., Sahin A.Z., Yilbas B.S. Thermodynamic analysis of a thermoelectric power generator in relation to geometric configuration device pins. *Energy Convers Manag* 2014;78:634–640. doi:10.1016/j.enconman.2013.11.029.
- [62] Lamba R., Kaushik S.C. Thermodynamic analysis of thermoelectric generator including influence of Thomson effect and leg geometry configuration. *Energy Convers Manag* 2017;144:388–398. doi:10.1016/j.enconman.2017.04.069.
- [63] Shi Y., Mei D., Yao Z., Wang Y., Liu H., Chen Z. Nominal power density analysis of thermoelectric pins with non-constant cross sections. *Energy Convers Manag* 2015;97:1–6. doi:10.1016/j.enconman.2015.02.046.
- [64] Fabián-Mijangos A., Min G., Alvarez-Quintana J. Enhanced performance thermoelectric module having asymmetrical legs. *Energy Convers Manag* 2017;148:1372–1381. doi:10.1016/j.enconman.2017.06.087.
- [65] Lin S., Yu J. Optimization of a trapezoid-type two-stage Peltier couples for thermoelectric cooling applications. *Int J Refrig* 2016;65:103–110. doi:10.1016/j.ijrefrig.2015.12.007.
- [66] Lamba R., Manikandan S., Kaushik S.C., Tyagi S.K. Thermodynamic modelling and performance optimization of trapezoidal thermoelectric cooler using genetic algorithm. *Therm Sci Eng Prog* 2018;6:236–250. doi:10.1016/j.tsep.2018.04.010.
- [67] Liu H.-B., Meng J.-H.H., Wang X.-D.D., Chen W.-H.H. A new design of solar thermoelectric generator with combination of segmented materials and asymmetrical legs. *Energy Convers Manag* 2018;175:11–20. doi:10.1016/j.enconman.2018.08.095.
- [68] Shittu S., Li G., Zhao X., Ma X., Akhlaghi Y.G., Ayodele E. Optimized high performance thermoelectric generator with combined segmented and asymmetrical legs under pulsed heat input power. *J Power Sources* 2019;428:53–66. doi:10.1016/j.jpowsour.2019.04.099.
- [69] Karana D.R., Sahoo R.R. Influence of geometric parameter on the performance of a new asymmetrical and segmented thermoelectric generator. *Energy* 2019;179:90–99. doi:10.1016/j.energy.2019.04.199.
- [70] Luo D., Wang R., Yu W., Zhou W. Performance evaluation of a novel thermoelectric module with BiSbTeSe-based material. *Appl Energy* 2019;238:1299–1311. doi:10.1016/j.apenergy.2019.01.139.
- [71] He W., Wang S., Zhang X., Li Y., Lu C. Optimization design method of thermoelectric generator based on exhaust gas parameters for recovery of engine waste heat. *Energy* 2015;91:1–9.

- [72] Lee H.S. Optimal design of thermoelectric devices with dimensional analysis. *Appl Energy* 2013;106:79–88. doi:10.1016/j.apenergy.2013.01.052.
- [73] Min G., Rowe D.M. Ring-structured thermoelectric module. *Semicond Sci Technol* 2007;22:880–883. doi:10.1088/0268-1242/22/8/009.
- [74] Bauknecht A., Steinert T., Spengler C., Suck G. Analysis of annular thermoelectric couples with nonuniform temperature distribution by means of 3-D multiphysics simulation. *J Electron Mater* 2013;42:1641–1646. doi:10.1007/s11664-012-2360-7.
- [75] Kaushik S.C., Manikandan S. The influence of Thomson effect in the energy and exergy efficiency of an annular thermoelectric generator. *Energy Convers Manag* 2015;103:200–207. doi:10.1016/j.enconman.2015.06.037.
- [76] Manikandan S., Kaushik S.C. Energy and exergy analysis of solar heat pipe based annular thermoelectric generator system. *Sol Energy* 2016;135:569–577. doi:10.1016/j.solener.2016.06.031.
- [77] Shen Z.G., Wu S.Y., Xiao L. Theoretical analysis on the performance of annular thermoelectric couple. *Energy Convers Manag* 2015;89:244–250. doi:10.1016/j.enconman.2014.09.071.
- [78] Ursell TS, Snyder GJ. Compatibility of segmented thermoelectric generators. In: *Int Conf Thermoelectr ICT, Proc 2002;2002–Janua:412–7*. doi:10.1109/ICT.2002.1190349.
- [79] Snyder G.J. Application of the compatibility factor to the design of segmented and cascaded thermoelectric generators. *Appl Phys Lett* 2004;84:2436–2438. doi:10.1063/1.1689396.
- [80] Snyder G.J., Ursell T.S. Thermoelectric efficiency and compatibility. *Phys Rev Lett* 2003;91. doi:10.1103/PhysRevLett.91.148301.
- [81] Sallehin N.Z.I.M., Yatim N.M., Suhaimi S. A review on fabrication methods for segmented thermoelectric structure. *AIP Conf Proc* 2018;1972:30003. doi:10.1063/1.5041224.
- [82] Hadjistassou C., Kyriakides E., Georgiou J. Designing high efficiency segmented thermoelectric generators. *Energy Convers Manag* 2013;66:165–172. doi:10.1016/j.enconman.2012.07.030.
- [83] Kim H.S., Kikuchi K., Itoh T., Iida T., Taya M. Design of segmented thermoelectric generator based on cost-effective and light-weight thermoelectric alloys. *Mater Sci Eng B Solid-State Mater Adv Technol* 2014;185:45–52. doi:10.1016/j.mseb.2014.02.005.
- [84] Shu G., Ma X., Tian H., Yang H., Chen T., Li X. Configuration optimization of the segmented modules in an exhaust-based thermoelectric generator for engine waste heat recovery. *Energy* 2018;160:612–624. doi:10.1016/j.energy.2018.06.175.
- [85] Ouyang Z., Li D. Design of segmented high-performance thermoelectric generators with cost in consideration. *Appl Energy* 2018;221:112–121. doi:10.1016/j.apenergy.2018.03.106.
- [86] Xiao J., Yang T., Li P., Zhai P., Zhang Q. Thermal design and management for performance optimization of solar thermoelectric generator. *Appl Energy* 2012;93:33–38.

- [87] Cheng K., Qin J., Jiang Y., Lv C., Zhang S., Bao W. Performance assessment of multi-stage thermoelectric generators on hypersonic vehicles at a large temperature difference. *Appl Therm Eng* 2018;130:1598–1609. doi:10.1016/j.applthermaleng.2017.11.057.
- [88] Cheng K., Qin J., Jiang Y., Zhang S., Bao W. Performance comparison of single- and multi-stage onboard thermoelectric generators and stage number optimization at a large temperature difference. *Appl Therm Eng* 2018;141:456–466. doi:10.1016/j.applthermaleng.2018.05.127.
- [89] Wang T.H., Wang Q.H., Leng C., Wang X.D. Parameter analysis and optimal design for two-stage thermoelectric cooler. *Appl Energy* 2015;154:1–12. doi:10.1016/j.apenergy.2015.04.104.
- [90] Lv H., Wang X.D., Meng J.H., Wang T.H., Yan W.M. Enhancement of maximum temperature drop across thermoelectric cooler through two-stage design and transient supercooling effect. *Appl Energy* 2016;175:285–292. doi:10.1016/j.apenergy.2016.05.035.
- [91] Owoyele O., Ferguson S., O'Connor B.T. Performance analysis of a thermoelectric cooler with a corrugated architecture. *Appl Energy* 2015;147:184–191. doi:10.1016/j.apenergy.2015.01.132.
- [92] Sun T., Peavey J.L., David Shelby M., Ferguson S., O'Connor B.T. Heat shrink formation of a corrugated thin film thermoelectric generator. *Energy Convers Manag* 2015;103:674–680. doi:10.1016/j.enconman.2015.07.016.
- [93] Liu K., Tang X., Liu Y., Yuan Z., Li J., Xu Z., et al. High-performance and integrated design of thermoelectric generator based on concentric filament architecture. *J Power Sources* 2018;393:161–168. doi:10.1016/j.jpowsour.2018.05.018.
- [94] Liu K., Tang X., Liu Y., Xu Z., Yuan Z., Li J., et al. Preparation and optimization of miniaturized radioisotope thermoelectric generator based on concentric filament architecture. *J Power Sources* 2018;407:14–22. doi:10.1016/j.jpowsour.2018.10.052.
- [95] Jia X., Gao Y. Optimal design of a novel thermoelectric generator with linear-shaped structure under different operating temperature conditions. *Appl Therm Eng* 2015;78:533–542. doi:10.1016/j.applthermaleng.2014.12.011.
- [96] Ali H., Yilbas B.S., Al-Sharafi A. Innovative design of a thermoelectric generator with extended and segmented pin configurations. *Appl Energy* 2017;187:367–379. doi:10.1016/j.apenergy.2016.11.050.
- [97] Jia X.D., Wang Y.J., Gao Y.W. Numerical simulation of thermoelectric performance of linear-shaped thermoelectric generators under transient heat supply. *Energy* 2017;130:276–285. doi:10.1016/j.energy.2017.04.072.
- [98] Ali H., Yilbas B.S. Innovative design of a thermoelectric generator of extended legs with tapering and segmented pin configuration: thermal performance analysis. *Appl Therm Eng* 2017;123:74–91. doi:10.1016/j.applthermaleng.2017.05.066.
- [99] Glatz W., Muntwyler S., Hierold C. Optimization and fabrication of thick flexible polymer based micro thermoelectric generator. *Sensors Actuators, A Phys* 2006;132:337–345.

- [100] Aranguren P., Roch A., Stepien L., Abt M., Von Lukowicz M., Dani I., et al. Optimized design for flexible polymer thermoelectric generators. *Appl Therm Eng* 2016;102:402–411. doi:10.1016/j.applthermaleng.2016.03.037.
- [101] Qing S., Rezanian A., Rosendahl L.A., Enkeshafi A.A., Gou X. Characteristics and parametric analysis of a novel flexible ink-based thermoelectric generator for human body sensor. *Energy Convers Manag* 2018;156:655–665. doi:10.1016/j.enconman.2017.11.065.
- [102] Karthikeyan V., Surjadi J.U., Wong J.C.K., Kannan V., Lam K.H., Chen X., et al. Wearable and flexible thin film thermoelectric module for multi-scale energy harvesting. *J Power Sources* 2020;455:227983. doi:10.1016/j.jpowsour.2020.227983.
- [103] Dunham M.T., Barako M.T., LeBlanc S., Asheghi M., Chen B., Goodson K.E. Power density optimization for micro thermoelectric generators. *Energy* 2015;93:2006–2017. doi:10.1016/j.energy.2015.10.032.
- [104] Dunham M.T., Barako M.T., Cornett J.E., Gao Y., Haidar S., Sun N., et al. Experimental characterization of microfabricated thermoelectric energy harvesters for smart sensor and wearable applications. *Adv Mater Technol* 2018;3:1–12. doi:10.1002/admt.201700383.
- [105] Liu S., Hu B., Liu D., Li F., Li J.F., Li B., et al. Micro-thermoelectric generators based on through glass pillars with high output voltage enabled by large temperature difference. *Appl Energy* 2018;225:600–610. doi:10.1016/j.apenergy.2018.05.056.
- [106] Shittu S., Li G., Zhao X., Akhlaghi Y.G., Ma X., Yu M. Comparative study of a concentrated photovoltaic-thermoelectric system with and without flat plate heat pipe. *Energy Convers Manag* 2019;193:1–14. doi:10.1016/j.enconman.2019.04.055.
- [107] Bjørk R., Christensen D.V., Eriksen D., Pryds N. Analysis of the internal heat losses in a thermoelectric generator. *Int J Therm Sci* 2014;85:12–20. doi:10.1016/j.ijthermalsci.2014.06.003.
- [108] Rezanian A., Rosendahl L.A., Yin H. Parametric optimization of thermoelectric elements footprint for maximum power generation. *J Power Sources* 2014;255:151–156. doi:10.1016/j.jpowsour.2014.01.002.
- [109] Shi Y., Zhu Z., Deng Y., Zhu W., Chen X., Zhao Y. A real-sized three-dimensional numerical model of thermoelectric generators at a given thermal input and matched load resistance. *Energy Convers Manag* 2015;101:713–720. doi:10.1016/j.enconman.2015.06.020.
- [110] Meng X., Suzuki R.O. Helical configuration for thermoelectric generation. *Appl Therm Eng* 2016;99:352–357. doi:10.1016/j.applthermaleng.2016.01.061.
- [111] Ming T., Yang W., Huang X., Wu Y., Li X., Liu J. Analytical and numerical investigation on a new compact thermoelectric generator. *Energy Convers Manag* 2017;132:261–271. doi:10.1016/j.enconman.2016.11.043.
- [112] Fernández-Yañez P., Armas O., Capetillo A., Martínez-Martínez S. Thermal analysis of a thermoelectric generator for light-duty diesel engines. *Appl Energy* 2018;226:690–702.

- [113] Ferreira-Teixeira S., Pereira A.M. Geometrical optimization of a thermoelectric device: numerical simulations. *Energy Convers Manag* 2018;169:217–227. doi:10.1016/j.enconman.2018.05.030.
- [114] Lee H., Sharp J., Stokes D., Pearson M., Priya S. Modeling and analysis of the effect of thermal losses on thermoelectric generator performance using effective properties. *Appl Energy* 2018;211:987–996. doi:10.1016/j.apenergy.2017.11.096.
- [115] Liao M., He Z., Jiang C., Fan X., Li Y., Qi F. A three-dimensional model for thermoelectric generator and the influence of Peltier effect on the performance and heat transfer. *Appl Therm Eng* 2018;133:493–500. doi:10.1016/j.applthermaleng.2018.01.080.
- [116] Wang X., Wang H., Su W., Mehmood F., Zhai J., Wang T., et al. Geometric structural design for lead tellurium thermoelectric power generation application. *Renew Energy* 2019;141:88–95. doi:10.1016/j.renene.2019.03.128.
- [117] Gong T., Gao L., Wu Y., Zhang L., Yin S., Li J., et al. Numerical simulation on a compact thermoelectric cooler for the optimized design. *Appl Therm Eng* 2019;146:815–825. doi:10.1016/j.applthermaleng.2018.10.047.
- [118] Kwan T.H., Wu X. Power and mass optimization of the hybrid solar panel and thermoelectric generators. *Appl Energy* 2016;165:297–307. doi:10.1016/j.apenergy.2015.12.016.
- [119] Khire R.A., Messac A., Van Dessel S. Design of thermoelectric heat pump unit for active building envelope systems. *Int J Heat Mass Transf* 2005;48:4028–4040. doi:10.1016/j.ijheatmasstransfer.2005.04.028.
- [120] Cai L., Li P., Luo Q., Zhai P., Zhang Q. Geometry optimization of a segmented thermoelectric generator based on multi-parameter and nonlinear optimization method. *J Electron Mater* 2017;46:1552–1566. doi:10.1007/s11664-016-5198-6.
- [121] Khanh D.V.K., Vasant P.M., Elamvazuthi I., Dieu V.N. Geometric optimisation of thermo-electric coolers using simulated annealing. *Int J Comput Sci Eng* 2017;14:279–289. doi:10.1504/IJCSE.2017.084164.
- [122] Cheng Y.H., Lin W.K. Geometric optimization of thermoelectric coolers in a confined volume using genetic algorithms. *Appl Therm Eng* 2005;25:2983–2997. doi:10.1016/j.applthermaleng.2005.03.007.
- [123] Lossec M., Multon B., Ben Ahmed H. Sizing optimization of a thermoelectric generator set with heatsink for harvesting human body heat. *Energy Convers Manag* 2013;68:260–265. doi:10.1016/j.enconman.2013.01.021.
- [124] Ibrahim A., Rahnamayan S., Vargas Martin M., Yilbas B. Multi-objective thermal analysis of a thermoelectric device: influence of geometric features on device characteristics. *Energy* 2014;77:305–317. doi:10.1016/j.energy.2014.08.041.
- [125] Takezawa A., Kitamura M. Geometrical design of thermoelectric generators based on topology optimization. *Int J Numer Methods Eng* 2012;90:1363–1392. doi:10.1002/nme.

- [126] Lundgaard C., Sigmund O. Design of segmented off-diagonal thermoelectric generators using topology optimization. *Appl Energy* 2019;236:950–960. doi:10.1016/j.apenergy.2018.12.021.
- [127] Lundgaard C., Sigmund O. Design of segmented thermoelectric Peltier coolers by topology optimization. *Appl Energy* 2019;239:1003–1013. doi:10.1016/j.apenergy.2019.01.247.
- [128] Kwan T.H., Wu X., Yao Q. Multi-objective genetic optimization of the thermoelectric system for thermal management of proton exchange membrane fuel cells. *Appl Energy* 2018;217:314–327. doi:10.1016/j.apenergy.2018.02.097.
- [129] Deb K., Member A., Pratap A., Agarwal S., Meyarivan T. A fast and elitist multi-objective genetic algorithm: NSGAII. *IEEE Trans Evol Comput* 2002;6:182–197.
- [130] Arora R., Kaushik S.C., Arora R. Multi-objective and multi-parameter optimization of two-stage thermoelectric generator in electrically series and parallel configurations through NSGA-II. *Energy* 2015;91:242–254. doi:10.1016/j.energy.2015.08.044.
- [131] Arora R., Kaushik S.C., Arora R. Thermodynamic modeling and multi-objective optimization of two stage thermoelectric generator in electrically series and parallel configuration. *Appl Therm Eng* 2016;103:1312–1323. doi:10.1016/j.applthermaleng.2016.05.009.
- [132] Lamba R., Kaushik S.C., Tyagi S.K. Geometric optimization of trapezoidal thermoelectric heat pump considering contact resistances through genetic algorithm. *Int J Energy Res* 2018;42:633–647. doi:10.1002/er.3845.
- [133] Jang J.Y., Tsai Y.C. Optimization of thermoelectric generator module spacing and spreader thickness used in a waste heat recovery system. *Appl Therm Eng* 2013;51:677–689. doi:10.1016/j.applthermaleng.2012.10.024.
- [134] Meng J.H., Zhang X.X., Wang X.D. Multi-objective and multi-parameter optimization of a thermoelectric generator module. *Energy* 2014;71:367–376. doi:10.1016/j.energy.2014.04.082.
- [135] Liu Z., Zhu S., Ge Y., Shan F., Zeng L., Liu W. Geometry optimization of two-stage thermoelectric generators using simplified conjugate-gradient method. *Appl Energy* 2017;190:540–552. doi:10.1016/j.apenergy.2017.01.002.
- [136] Huang Y.X., Wang X.D., Cheng C.H., Lin D.T.W. Geometry optimization of thermoelectric coolers using simplified conjugate-gradient method. *Energy* 2013;59:689–697. doi:10.1016/j.energy.2013.06.069.
- [137] Kishore R.A., Sanghadasa M., Priya S. Optimization of segmented thermoelectric generator using Taguchi and ANOVA techniques. *Sci Rep* 2017;7:1–15. doi:10.1038/s41598-017-16372-8.
- [138] Kishore R.A., Kumar P., Priya S. A comprehensive optimization study on Bi₂Te₃-based thermoelectric generators using the Taguchi method. *Sustain Energy Fuels* 2018;2:175–190. doi:10.1039/c7se00437k.
- [139] Chen W.H., Huang S.R., Lin Y.L. Performance analysis and optimum operation of a thermoelectric generator by Taguchi method. *Appl Energy* 2015;158:44–54. doi:10.1016/j.apenergy.2015.08.025.

- [140] Soprani S., Haertel J.H.K., Lazarov B.S., Sigmund O., Engelbrecht K. A design approach for integrating thermoelectric devices using topology optimization. *Appl Energy* 2016;176:49–64. doi:10.1016/j.apenergy.2016.05.024.
- [141] Heghmanns A., Beitelschmidt M. Parameter optimization of thermoelectric modules using a genetic algorithm. *Appl Energy* 2015;155:447–454. doi:10.1016/j.apenergy.2015.06.034.
- [142] Chen W.H., Wu P.H., Lin Y.L. Performance optimization of thermoelectric generators designed by multi-objective genetic algorithm. *Appl Energy* 2018;209:211–223. doi:10.1016/j.apenergy.2017.10.094.
- [143] Ge Y., Liu Z., Sun H., Liu W. Optimal design of a segmented thermoelectric generator based on three-dimensional numerical simulation and multi-objective genetic algorithm. *Energy* 2018;147:1060–1069. doi:10.1016/j.energy.2018.01.099.
- [144] Meng J.-H., Wu H.-C., Wang T.-H. Optimization of two-stage combined thermoelectric devices by a three-dimensional multi-physics model and multi-objective genetic algorithm. *Energies* 2019;12:2832.
- [145] Sun H., Ge Y., Liu W., Liu Z. Geometric optimization of two-stage thermoelectric generator using genetic algorithms and thermodynamic analysis. *Energy* 2019;171:37–48. doi:10.1016/j.energy.2019.01.003.
- [146] Sun H., Gil S.U., Liu W., Liu Z. Structure optimization and exergy analysis of a two-stage TEC with two different connections. *Energy* 2019;180:175–191. doi:10.1016/j.energy.2019.05.077.
- [147] Shittu S., Li G., Xuan Q., Zhao X., Ma X., Cui Y. Electrical and mechanical analysis of a segmented solar thermoelectric generator under non-uniform heat flux. *Energy* 2020;199:117433. doi:10.1016/j.energy.2020.117433.
- [148] Clin T., Turenne S., Vasilevskiy D., Masut R.A. Numerical simulation of the thermomechanical behavior of extruded bismuth telluride alloy module. *J Electron Mater* 2009;38:994–1001. doi:10.1007/s11664-009-0756-9.
- [149] Turenne S., Clin T., Vasilevskiy D., Masut R.A. Finite element thermomechanical modeling of large area thermoelectric generators based on bismuth telluride alloys. *J Electron Mater* 2010;39:1926–1933. doi:10.1007/s11664-009-1049-z.
- [150] Gao J.-L., Du Q.-G., Zhang X.-D., Jiang X.-Q. Thermal stress analysis and structure parameter selection for a Bi₂Te₃-based thermoelectric module. *J Electron Mater* 2011;40:884–888. doi:10.1007/s11664-011-1611-3.
- [151] Al-Merbaty A.S., Yilbas B.S., Sahin A.Z. Thermodynamics and thermal stress analysis of thermoelectric power generator: influence of pin geometry on device performance. *Appl Therm Eng* 2013;50:683–692. doi:10.1016/j.applthermaleng.2012.07.021.
- [152] Chen G., Mu Y., Zhai P., Li G., Zhang Q. An investigation on the coupled thermal-mechanical-electrical response of automobile thermoelectric materials and devices. *J Electron Mater* 2013;42:1762–1770. doi:10.1007/s11664-012-2422-x.

- [153] Mu Y., Chen G., Yu R., Li G., Zhai P., Li P. Effect of geometric dimensions on thermoelectric and mechanical performance for Mg₂Si-based thermoelectric unicouple. *Mater Sci Semicond Process* 2014;17:21–26. doi:10.1016/j.mssp.2013.08.009.
- [154] Jia X., Gao Y. Estimation of thermoelectric and mechanical performances of segmented thermoelectric generators under optimal operating conditions. *Appl Therm Eng* 2014;73:333–340. doi:10.1016/j.applthermaleng.2014.07.069.
- [155] Jia X., Guo Q. Design study of Bismuth-Telluride-based thermoelectric generators based on thermoelectric and mechanical performance. *Energy* 2020;190:116226. doi:10.1016/j.energy.2019.116226.
- [156] Erturun U., Erermis K., Mossi K. Effect of various leg geometries on thermo-mechanical and power generation performance of thermoelectric devices. *Appl Therm Eng* 2014;73:128–141. doi:10.1016/j.applthermaleng.2014.07.027.
- [157] Erturun U., Mossi K. Thermoelectric devices with rotated and coaxial leg configurations: numerical analysis of performance. *Appl Therm Eng* 2015;85:304–312. doi:10.1016/j.applthermaleng.2015.04.010.
- [158] Erturun U., Erermis K., Mossi K. Influence of leg sizing and spacing on power generation and thermal stresses of thermoelectric devices. *Appl Energy* 2015;159:19–27. doi:10.1016/j.apenergy.2015.08.112.
- [159] Ming T., Wang Q., Peng K., Cai Z., Yang W., Wu Y., et al. The influence of non-uniform high heat flux on thermal stress of thermoelectric power generator. *Energies* 2015;8:12584–12602. doi:10.3390/en8112332.
- [160] Ming T., Yang W., Wu Y., Xiang Y., Huang X., Cheng J., et al. Numerical analysis on the thermal behavior of a segmented thermoelectric generator. *Int J Hydrogen Energy* 2017;42:3521–3535. doi:10.1016/j.ijhydene.2016.11.021.
- [161] Wu Y., Ming T., Li X., Pan T., Peng K., Luo X. Numerical simulations on the temperature gradient and thermal stress of a thermoelectric power generator. *Energy Convers Manag* 2014;88:915–927. doi:10.1016/j.enconman.2014.08.069.
- [162] Bakhtiaryfard L., Chen Y.S. Design and analysis of a thermoelectric module to improve the operational life. *Adv Mech Eng* 2015;7:1–22. doi:10.1155/2014/152419.
- [163] Yilbas B.S., Akhtar S.S., Sahin A.Z. Thermal and stress analyses in thermoelectric generator with tapered and rectangular pin configurations. *Energy* 2016;114:52–63. doi:10.1016/j.energy.2016.07.168.
- [164] Karri N.K., Mo C. Structural reliability evaluation of thermoelectric generator modules: influence of end conditions, leg geometry, metallization, and processing temperatures. *J Electron Mater* 2018;47:6101–6120. doi:10.1007/s11664-018-6505-1.
- [165] Karri N.K., Mo C. Reliable thermoelectric module design under opposing requirements from structural and thermoelectric considerations. *J Electron Mater* 2018;47:3127–3135.

- [166] Fan S., Gao Y. Numerical simulation on thermoelectric and mechanical performance of annular thermoelectric generator. *Energy* 2018;150:38–48. doi:10.1016/j.energy.2018.02.124.
- [167] Ibeagwu O.I. Modelling and comprehensive analysis of TEGs with diverse variable leg geometry. *Energy* 2019;180:90–106. doi:10.1016/j.energy.2019.05.088.
- [168] Gong T., Wu Y., Gao L., Zhang L., Li J., Ming T. Thermo-mechanical analysis on a compact thermoelectric cooler. *Energy* 2019;172:1211–1224. doi:10.1016/j.energy.2019.02.014.
- [169] Gong T., Gao L., Wu Y., Tan H., Qin F., Ming T. Transient thermal stress analysis of a thermoelectric cooler under pulsed thermal loading. *Appl Therm Eng* 2019;162:114240. doi:10.1016/j.applthermaleng.2019.114240.
- [170] He R., Schierning G., Nielsch K. Thermoelectric devices: a review of devices, architectures, and contact optimization. *Adv Mater Technol* 2018;3. doi:10.1002/admt.201700256.
- [171] Shittu S., Li G., Zhao X., Zhou J., Ma X. Experimental study and exergy analysis of photovoltaic-thermoelectric with flat plate micro-channel heat pipe. *Energy Convers Manag* 2020;207:112515. doi:10.1016/j.enconman.2020.112515.
- [172] Ebling D., Bartholomé K., Bartel M., Jäggle M. Module geometry and contact resistance of thermoelectric generators analyzed by multiphysics simulation. *J Electron Mater* 2010;39:1376–1380. doi:10.1007/s11664-010-1331-0.
- [173] Gomez M., Reid R., Ohara B., Lee H. Influence of electrical current variance and thermal resistances on optimum working conditions and geometry for thermoelectric energy harvesting. *J Appl Phys* 2013;113. doi:10.1063/1.4802668.
- [174] Fabian-Mijangos A, Alvarez-Quintana J. Thermoelectric devices: influence of the legs geometry and parasitic contact resistances on ZT. In: Aranguren P, editor. *Bringing Thermoelectr. into Real.*; 2018. doi:10.5772/intechopen.75790.
- [175] Massaguer A., Massaguer E., Comamala M., Pujol T., González J.R., Cardenas M.D., et al. A method to assess the fuel economy of automotive thermoelectric generators. *Appl Energy* 2018;222:42–58. doi:10.1016/j.apenergy.2018.03.169.
- [176] Höglblom O., Andersson R. Analysis of thermoelectric generator performance by use of simulations and experiments. *J Electron Mater* 2014;43:2247–2254. doi:10.1007/s11664-014-3020-x.
- [177] Luo Y., Kim C.N. Effects of the cross-sectional area ratios and contact resistance on the performance of a cascaded thermoelectric generator. *Int J Energy Res* 2019;43:2172–2187. doi:10.1002/er.4426.
- [178] Ouyang Z., Li D. Modelling of segmented high-performance thermoelectric generators with effects of thermal radiation, electrical and thermal contact resistances. *Sci Rep* 2016;6:1–12. doi:10.1038/srep24123.

- [179] Gupta R.P., McCarty R., Sharp J. Practical contact resistance measurement method for bulk Bi₂Te₃-based thermoelectric devices. *J Electron Mater* 2014;43:1608–1612. doi:10.1007/s11664-013-2806-6.
- [180] Pietrzyk K., Ohara B., Watson T., Gee M., Avalos D., Lee H. Thermoelectric module design strategy for solid-state refrigeration. *Energy* 2016;114:823–832. doi:10.1016/j.energy.2016.08.058.
- [181] Kim Y., Yoon G., Park S.H. Direct contact resistance evaluation of thermoelectric legs. *Exp Mech* 2016;56:861–869. doi:10.1007/s11340-016-0131-8.
- [182] Sun D., Liu G., Shen L., Chen H., Yao Y., Jin S. Modeling of high power light-emitting diode package integrated with micro-thermoelectric cooler under various interfacial and size effects. *Energy Convers Manag* 2019;179:81–90. doi:10.1016/j.enconman.2018.10.063.
- [183] Li G., Zhang G., He W., Ji J., Lv S., Chen X., et al. Performance analysis on a solar concentrating thermoelectric generator using the micro-channel heat pipe array. *Energy Convers Manag* 2016;112:191–198. doi:10.1016/j.enconman.2016.01.025.
- [184] He W., Su Y., Wang Y.Q., Riffat S.B., Ji J. A study on incorporation of thermoelectric modules with evacuated-tube heat-pipe solar collectors. *Renew Energy* 2012;37:142–149. doi:10.1016/j.renene.2011.06.002.
- [185] Lv S., He W., Hu D., Zhu J., Li G., Chen H., et al. Study on a high-performance solar thermoelectric system for combined heat and power. *Energy Convers Manag* 2017;143:459–469. doi:10.1016/j.enconman.2017.04.027.
- [186] Cao Q., Luan W., Wang T. Performance enhancement of heat pipes assisted thermoelectric generator for automobile exhaust heat recovery. *Appl Therm Eng* 2018;130:1472–1479. doi:10.1016/j.applthermaleng.2017.09.134.
- [187] Li G., Ji J., Zhang G., He W., Chen X., Chen H. Performance analysis on a novel micro-channel heat pipe evacuated tube solar collector-incorporated thermoelectric generation. *Int J Energy Res* 2016;40:2117–2127. doi:10.1002/er.3589.
- [188] Wu S., Ding Y., Zhang C., Xu D. Improving the performance of a thermoelectric power system using a flat-plate heat pipe. *Chinese J Chem Eng* 2018;27:44–53. doi:10.1002/bit.260470306.
- [189] Asaadi S., Khalilarya S., Jafarmadar S. Numerical study on the thermal and electrical performance of an annular thermoelectric generator under pulsed heat power with different types of input functions. *Energy Convers Manag* 2018;167:102–112. doi:10.1016/j.enconman.2018.04.085.
- [190] Yamashita O., Odahara H., Satou K. Energy conversion efficiency of a thermoelectric generator under the periodically alternating temperature gradients. *J Appl Phys* 2007;101. doi:10.1063/1.2425005.
- [191] Yazdanshenas E., Rezania A., Karami Rad M., Rosendahl L. Electrical response of thermoelectric generator to geometry variation under transient thermal boundary condition. *J Renew Sustain Energy* 2018;10. doi:10.1063/1.5040166.
- [192]

Ruiz-Ortega P.E., Olivares-Robles M.A., Enciso-Montes de Oca O.Y. Segmented thermoelectric generator under variable pulsed heat input power. *Entropy* 2019;21:1–16. doi:10.3390/e21100929.

[193] Ben Abdallah G., Besbes S., Ben Aissia H., Jay J. Analysis of the effect of a pulsed heat flux on the performance improvements of a thermoelectric generator. *Appl Therm Eng* 2019;158:113728. doi:10.1016/j.applthermaleng.2019.113728.

[194] Yan Y., Malen J.A. Periodic heating amplifies the efficiency of thermoelectric energy conversion. *Energy Environ Sci* 2013;6:1267–1273. doi:10.1039/c3ee24158k.

[195] Chen L., Lee J. Effect of pulsed heat power on the thermal and electrical performances of a thermoelectric generator. *Appl Energy* 2015;150:138–149. doi:10.1016/j.apenergy.2015.04.009.

[196] Snyder G.J., Fleurial J.P., Caillat T., Yang R., Chen G. Supercooling of Peltier cooler using a current pulse. *J Appl Phys* 2002;92:1564–1569. doi:10.1063/1.1489713.

[197] Thonhauser T., Mahan G.D., Zikatanov L., Roe J. Improved supercooling in transient

Highlights

- Detailed review of thermoelectric geometry and structure optimization are presented.
- Thermal stress studies on thermoelectric generators and coolers are reviewed.
- Three-dimensional and multi-objective optimization studies are reviewed.
- Future research directions on thermoelectric geometry optimization are presented.

Queries and Answers

Query: Your article is registered as a regular item and is being processed for inclusion in a regular issue of the journal. If this is NOT correct and your article belongs to a Special Issue/Collection please contact J.Shanmugam@elsevier.com immediately prior to returning your corrections.

Answer: Yes

Query: The author names have been tagged as given names and surnames (surnames are highlighted in teal color). Please confirm if they have been identified correctly.

Answer: Yes

Query: Please check the address for the corresponding author that has been added here, and correct if necessary.

Answer: *Corresponding authors at: Centre for Sustainable Energy Technologies, University of Hull, HU6 7RX, UK (G. Li); (X. Zhao).

E-mail addresses: Guiqiang.Li@hull.ac.uk (G.Li); Xudong.Zhao@hull.ac.uk (X.Zhao)

Query: Have we correctly interpreted the following funding source(s) and country names you cited in your article:

EU Marie Curie, United Kingdom? /

Answer: Yes